New numerical model to couple incompressible Navier-Stokes with a Gross-Pitaevskii superfluid

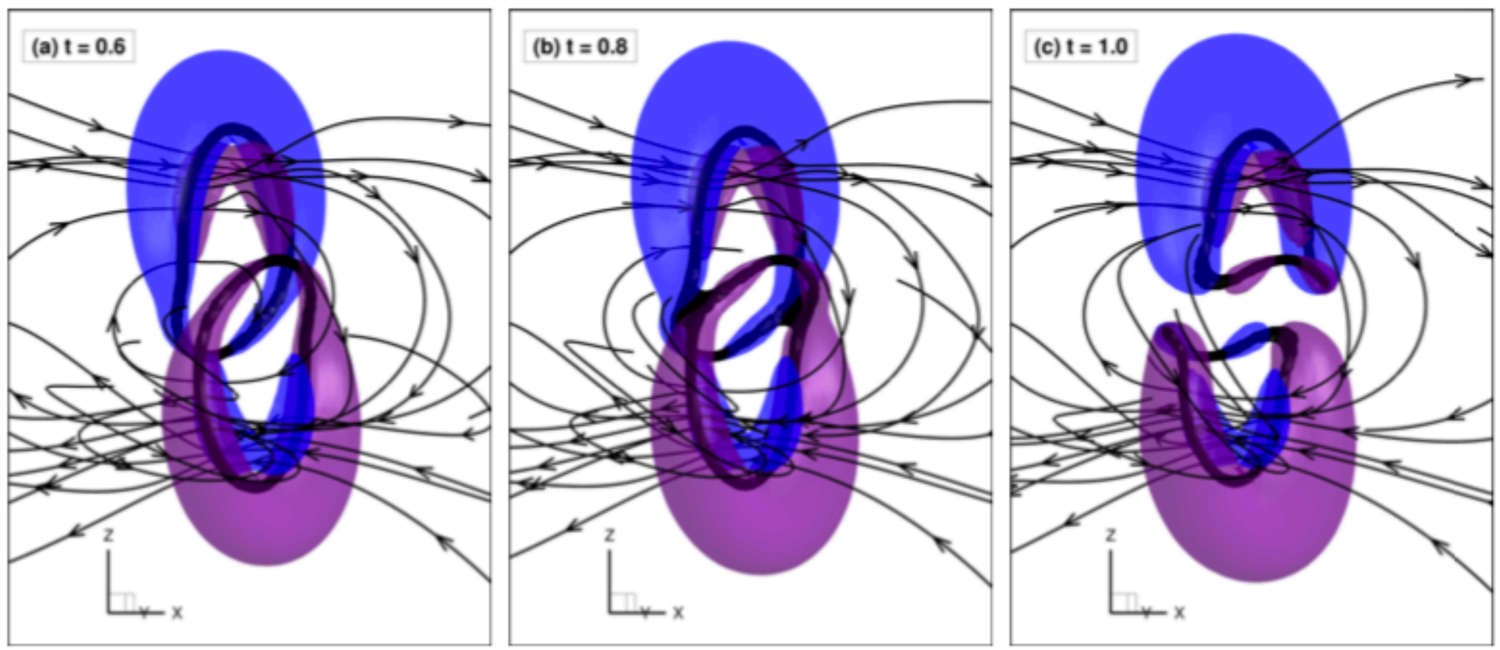

Marc Brachet
LPENS

Bridging Classical and Quantum Turbulence
3-15 Jul 2023 Cargèse, Corsica (France)

Work done in collaboration with

- Georges Sadaka
- Zhentong Zhang
- Victor Kalt
- Ionut Danaila

The talk is about this paper :

Coupling Navier-Stokes and Gross-Pitaevskii equations for the numerical simulation of two-fluid quantum flows

Marc Brachet [a], Georges Sadaka [b], Zhentong Zhang [b], Victor Kalt [b], Ionut Danaila [b,*]

Journal of Computational Physics 488 (2023) 112193

Why try to couple incompressible Navier-Stokes with a Gross-Pitaevskii superfluid?

The talk will start with a general introduction:

- Introduction: Burgers; Euler (compressible and inc.); Gross-Pitaevskii Equation (GPE=Nonlinear Schrödinger) Madelung's transformation. Example: Quantum shocks in (linear) Schrödinger Equation.
- Some orders of magnitude.
- Physical motivations

Then I will present:

- Building up the model
- The uncoupled GP and NS equations
- The regularized superfluid velocity field
- Determination of the slip velocity field and volume friction force
- Definition of coupling terms in the GP equation
- Numerical coupling algorithm
- Numerical results
- 2D superfluid vortex dipole: determination of model coefficients by comparing one-way GP-NS coupling to analytical solutions
- Results for two-way GP-NS coupling for the vortex dipole
- Results for 3D superfluid vortex rings and reconnection
- Conclusion

Introduction. Hydrodynamic Systems

- Perfect fluids
- Superfluids
- Simple examples using Burgers equation

What is a perfect fluid?

- Real classical fluids are viscous and conduct heat
- Perfect fluids are idealized models in which these mechanisms are neglected
- Perfect fluids have zero shear stresses, viscosities, and heat conduction
- Good approximation in some physical cases

Euler Equations

- A perfect fluid can be completely characterized by its velocity and two independent thermodynamic variables.

- If only one thermodynamic variable exists (e.g. isentropic perfect fluid) the fluid is barotropic.

- The density of a barotropic fluid is a function of pressure only.

Barotropic Euler equations

$$\boxed{\begin{aligned} \partial_t \mathbf{v} + \mathbf{v} \cdot \nabla \mathbf{v} &= -\frac{1}{\rho} \nabla p \\ \partial_t \rho + \nabla (\rho \mathbf{v}) &= 0 \end{aligned}}$$

Barotropic: $p(\mathbf{x}, t) = f(\rho(\mathbf{x}, t))$

Acoustic propagation: $c = \sqrt{\frac{\partial p}{\partial \rho}}$

Note that the system is time-reversible:

$$t \to -t \; ; \mathbf{v} \to -\mathbf{v} \; ; \rho \to \rho \; ; p \to p$$

Two useful limits

1. incompressible:

$$\rho = cte \qquad c \rightarrow \infty$$

$$\nabla \mathbf{v} = 0$$

There is no equation of state and p is determined by maintaining the incompressibility

2. irrotational:

$$\nabla \times \mathbf{v} = 0$$

$$c = \sqrt{\frac{\partial p}{\partial \rho}}$$

$$\mathbf{v} = \nabla \phi$$

Only compressible modes...

Variational approach

- For the general case see e.g. : R. L. Seliger and G. B. Whitham, Variational Principles in Continuum Mechanics, Proc. R. Soc. Lond. A. 1968 305 1-25.

- Here I'll show how to deal only with the compressible irrotational case..

Irrotational case

$$\mathcal{L} = \rho\phi_t + \frac{\rho(\nabla\phi)^2}{2} + g(\rho)$$

$$\frac{\delta\mathcal{L}}{\delta\phi} = 0 \rightarrow \rho_t + \nabla(\rho(\nabla\phi)) = 0$$

define:

$$\mathbf{v} = \nabla\phi$$

$$\rho g'' = p'$$

$$\frac{\delta\mathcal{L}}{\delta\rho} = 0 \rightarrow \phi_t + \frac{(\nabla\phi)^2}{2} + g' = 0$$

taking the gradient of the last equation:

$$\mathbf{v}_t + \mathbf{v}\cdot\nabla\mathbf{v} = -\nabla g' \quad = -\frac{\nabla p}{\rho}$$

What is a superfluid?
Is it just an Eulerian perfect fluid?

No! Superfluids obey the Gross-Pitaevskii equation (GPE)

The quantum nature of the GPE does disturb some classical traditions of fluid mechanics. This often makes it unpopular…

The Gross-Pitaeveski Equation (GPE)

$$\boxed{\begin{gathered} i\hbar\partial_t\Psi = -\frac{\hbar^2}{2m}\nabla^2\Psi + g|\Psi|^2\Psi \\ \Psi = \sqrt{\rho/m}\exp i\frac{m}{\hbar}\Phi \end{gathered}}$$

- Describes a superfluid Bose-Einstein condensate at zero temperature
- Applies to a complex field
- Madelung's transformation gives hydrodynamical form
- Contains quantum vortices with quantized velocity circulation h/m

Variatitional formulation of the GPE

$$\mathcal{L} = -i\hbar\bar{\Psi}\partial_t\Psi + \frac{\hbar^2|\nabla\Psi|^2}{2m} + \frac{g|\Psi|^4}{2}$$

$$\Psi = \sqrt{\rho/m}\exp i\frac{m}{\hbar}\Phi$$

$$\boxed{\mathcal{L} = \rho\partial_t\Phi + \frac{\rho\nabla\Phi^2}{2} + \frac{g\rho^2}{2m^2} + \frac{\hbar^2(\nabla\sqrt{\rho})^2}{2m^2}}$$

Contrast and compare with Euler Equation Lagrangian:

$$\boxed{\mathcal{L} = \rho\phi_t + \frac{\rho(\nabla\phi)^2}{2} + g(\rho)}$$

GPE and Madelung

$$i\hbar\partial_t\Psi = -\frac{\hbar^2}{2m}\nabla^2\Psi + g|\Psi|^2\Psi$$

$$\psi(\mathbf{x},t) = \sqrt{\frac{\rho(\mathbf{x},t)}{m}}\exp\left[i\frac{m}{\hbar}\phi(\mathbf{x},t)\right], \qquad \mathbf{v} = \boldsymbol{\nabla}\phi$$

Speed of sound $\quad c = \sqrt{g|A_0|^2/m}$

Coherence length $\quad \xi = \sqrt{\hbar^2/2m|A_\mathbf{0}|^2 g}.$

$$\frac{\partial\rho}{\partial t} + \boldsymbol{\nabla}\cdot(\rho\,\boldsymbol{\nabla}\,\phi) = 0, \qquad \frac{\partial\phi}{\partial t} + \frac{1}{2}(\nabla\phi)^2 = c^2(1-\rho) + c^2\xi^2\frac{\Delta\sqrt{\rho}}{\sqrt{\rho}}.$$

Continuity and Bernoulli equations for a compressible fluid

Irrotational fluid, except near nodal lines of ψ = superfluid vortices, with quantum of circulation $\Gamma = 4\pi c\xi/\sqrt{2}$, which can naturally reconnect in this model.

Energies

The GPE conserves the total energy E, which can be decomposed as [24, 25]: $E = E_{\rm kin} + E_{\rm int} + E_{\rm q}$, with $E_{\rm kin} = \langle|\sqrt{\rho}\mathbf{v}|^2/2\rangle$, $E_{\rm int} = \langle c^2(\rho-1)^2/2\rangle$ and $E_{\rm q} = \langle c^2\xi^2|\nabla\sqrt{\rho}|^2\rangle$. The kinetic energy $E_{\rm kin}$ can be also decomposed into compressible $E^{\rm c}_{\rm kin}$ and incompressible $E^{\rm i}_{\rm kin}$ components, using $(\sqrt{\rho}\mathbf{v}) = (\sqrt{\rho}\mathbf{v})^{\rm c} + (\sqrt{\rho}\mathbf{v})^{\rm i}$ with $\nabla\cdot(\sqrt{\rho}\mathbf{v})^{\rm i} = 0$.

- See e.g. Nore, et al., Phys. Rev. Lett. 78, 3896, 1997
- Parsesval's theorem yields definition of energy spectra

1D Burgers equation,GPE and Madelung’s transformation

- Euler, irrotational case with zero pressure is called inviscid Burgers
- In this case, the GPE reduces to the (linear) Schrödinger equation
- Madelung transforms yields inviscid Burgers with an extra quantum pressure term
- In what immediately follows, we will compare the (slightly) viscous 1D Burgers case with the quantum case

Viscous Burgers

$$\partial_t \phi + \frac{1}{2}(\partial_x \phi)^2 = \nu \partial_{xx} \phi$$

$$\phi(t=0) = -\cos x$$

$$v = \partial_x \phi$$

Pseudospectral calculation

$\nu = 0.006136$

$\frac{2}{3}$ dealiasing 1024 grid points

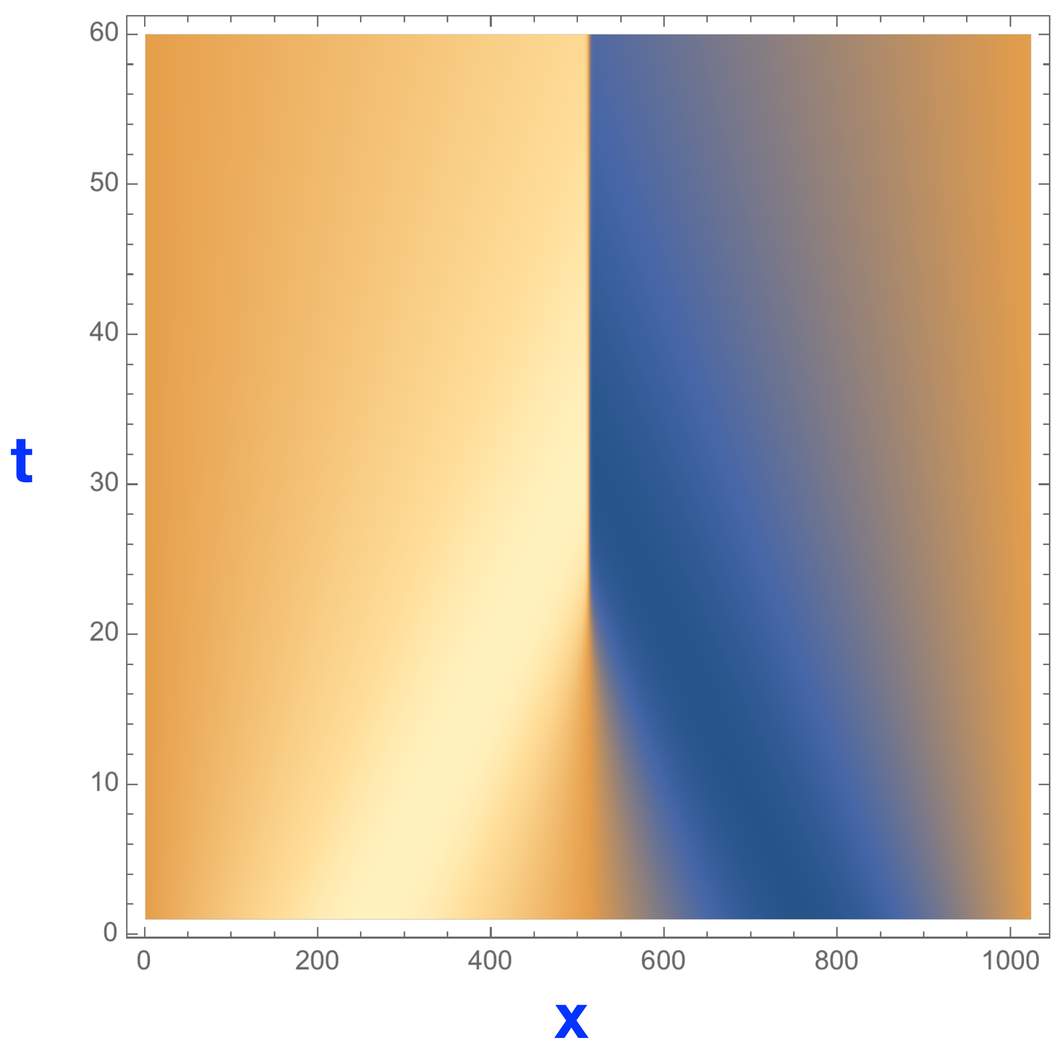

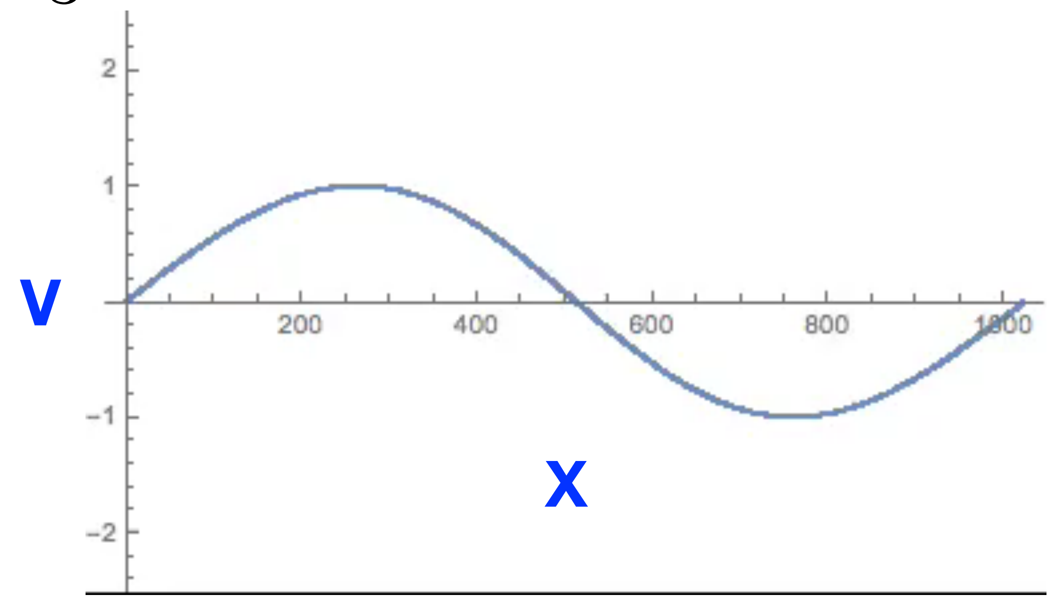

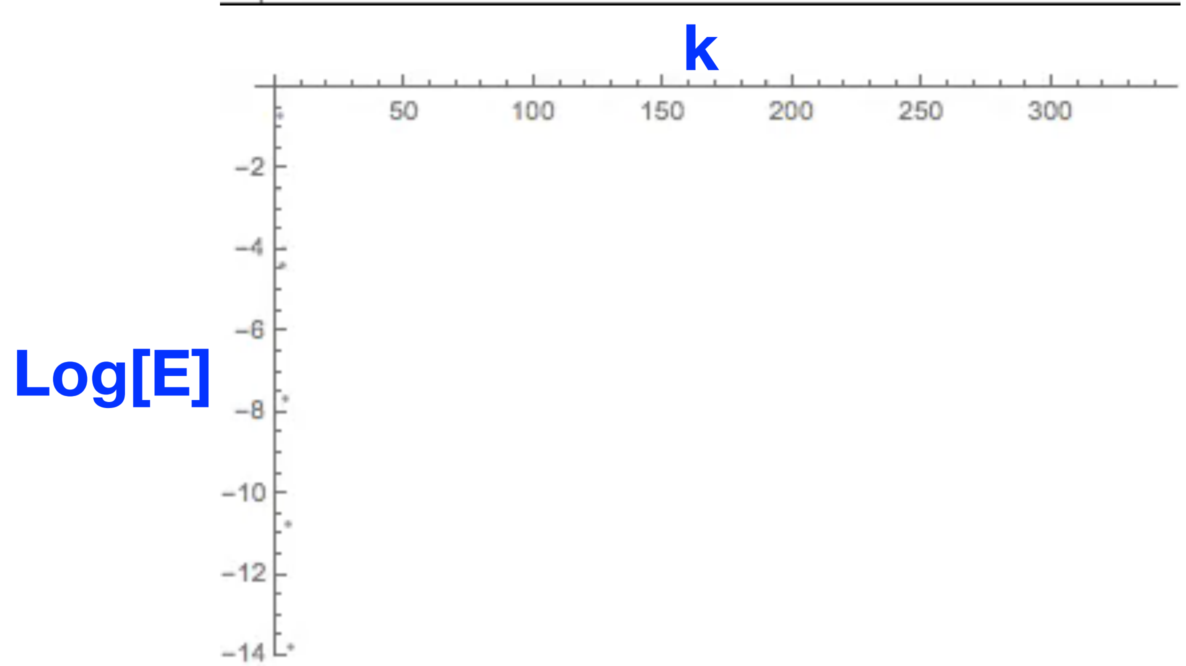

Quantum shocks in (linear) GPE

Schrödinger equation: $i\partial_t \psi = -\frac{\epsilon}{2}\partial_{xx}\psi$

Madelung's transformation: $\psi = \rho^{1/2} \exp i\frac{\phi}{\epsilon}$

Equations of motion:

$$\partial_t \phi + \frac{1}{2}(\partial_x \phi)^2 = \frac{\epsilon^2 \partial_{xx}\sqrt{\rho}}{2\sqrt{\rho}}$$

$$\partial_t \rho + \partial_x(\rho \partial_x \phi) = 0$$

Initial data

$$\phi(t=0) = -\cos x$$

$$\rho(t=0) = 1$$

$$v = \partial_x \phi$$

$$\epsilon = 0.0117188$$

Single QFD shock

Density

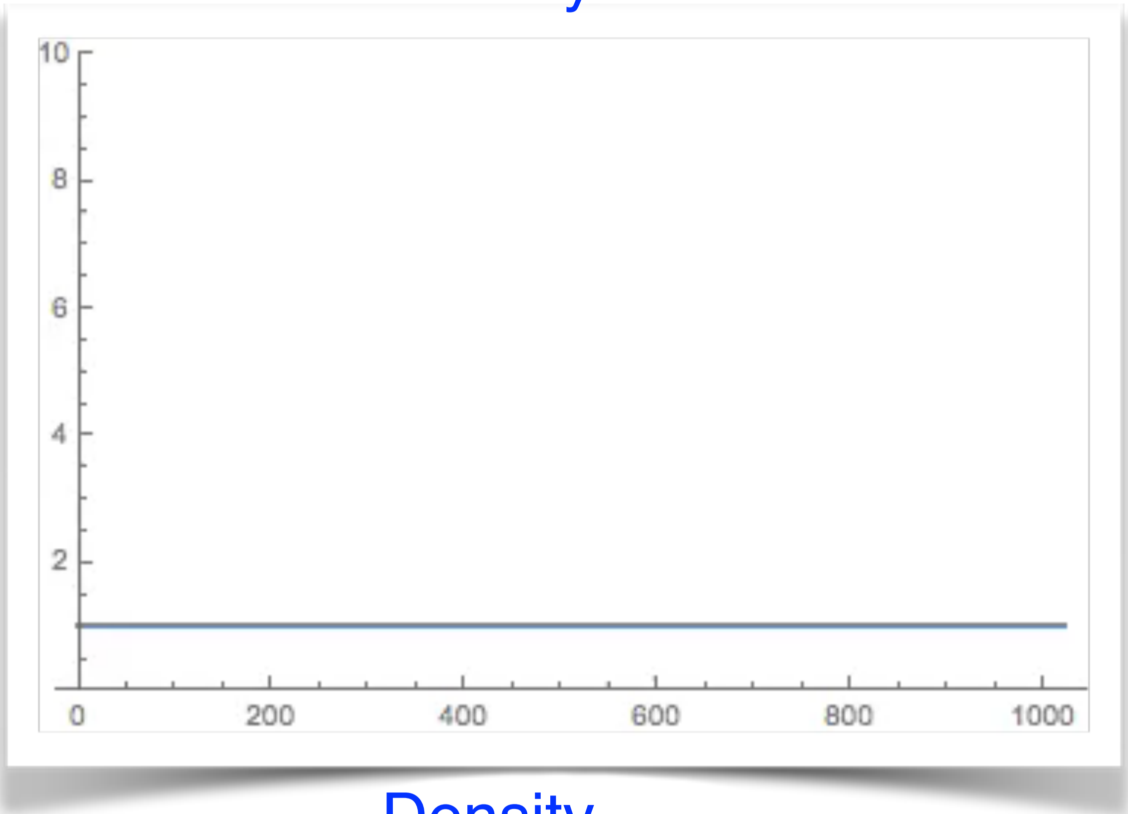

Velocity

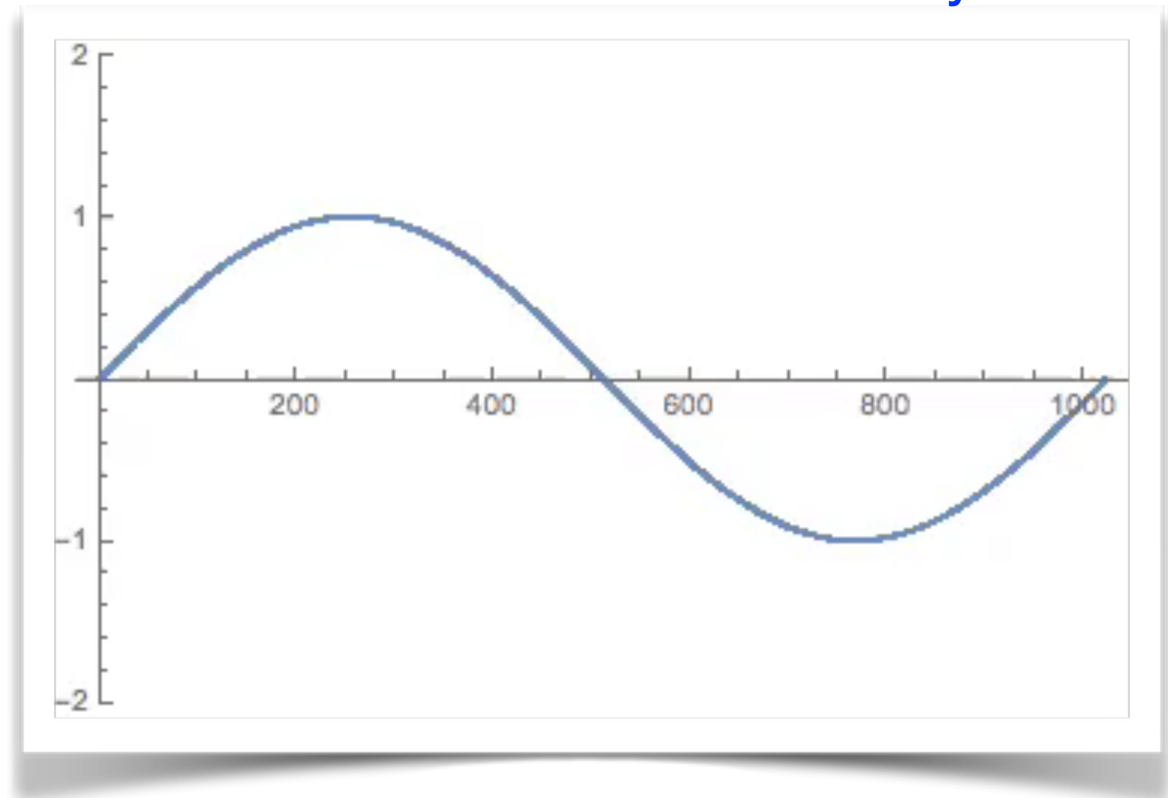

Density

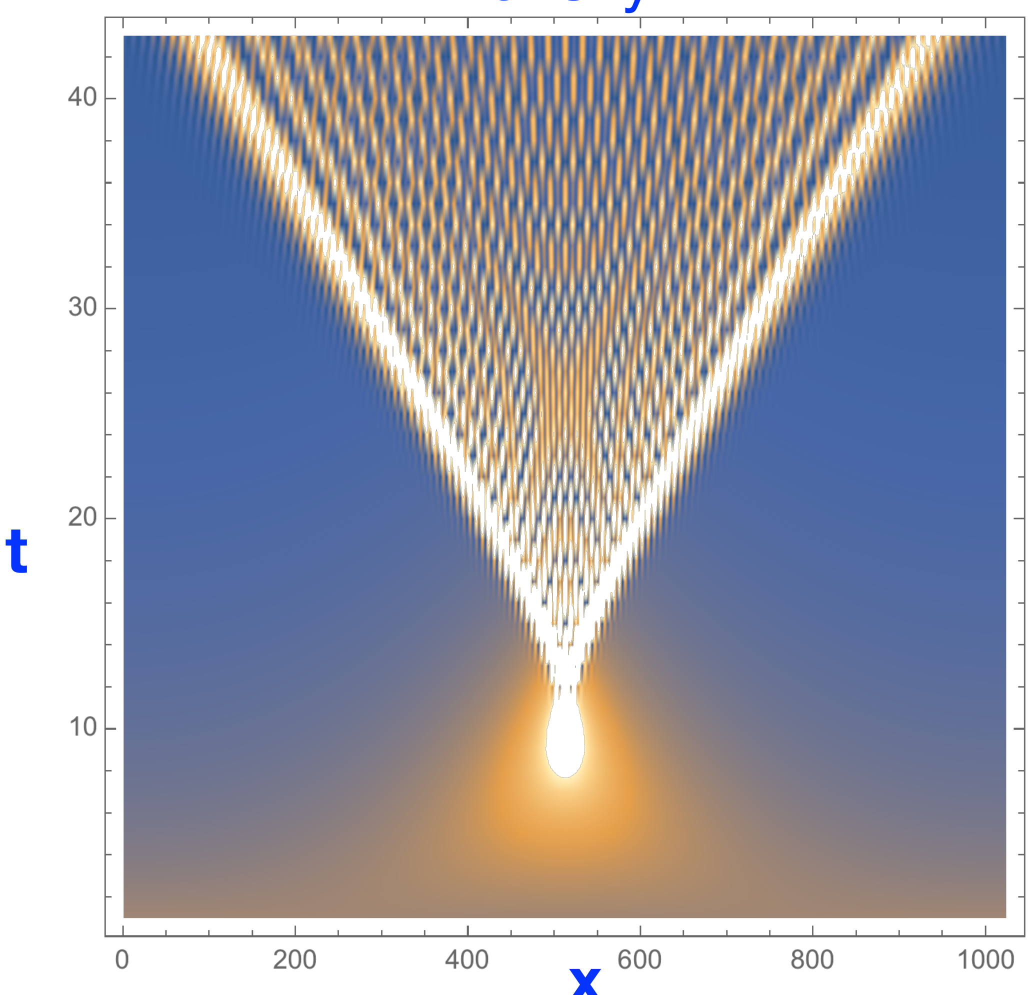

Momentum=Density * Velocity

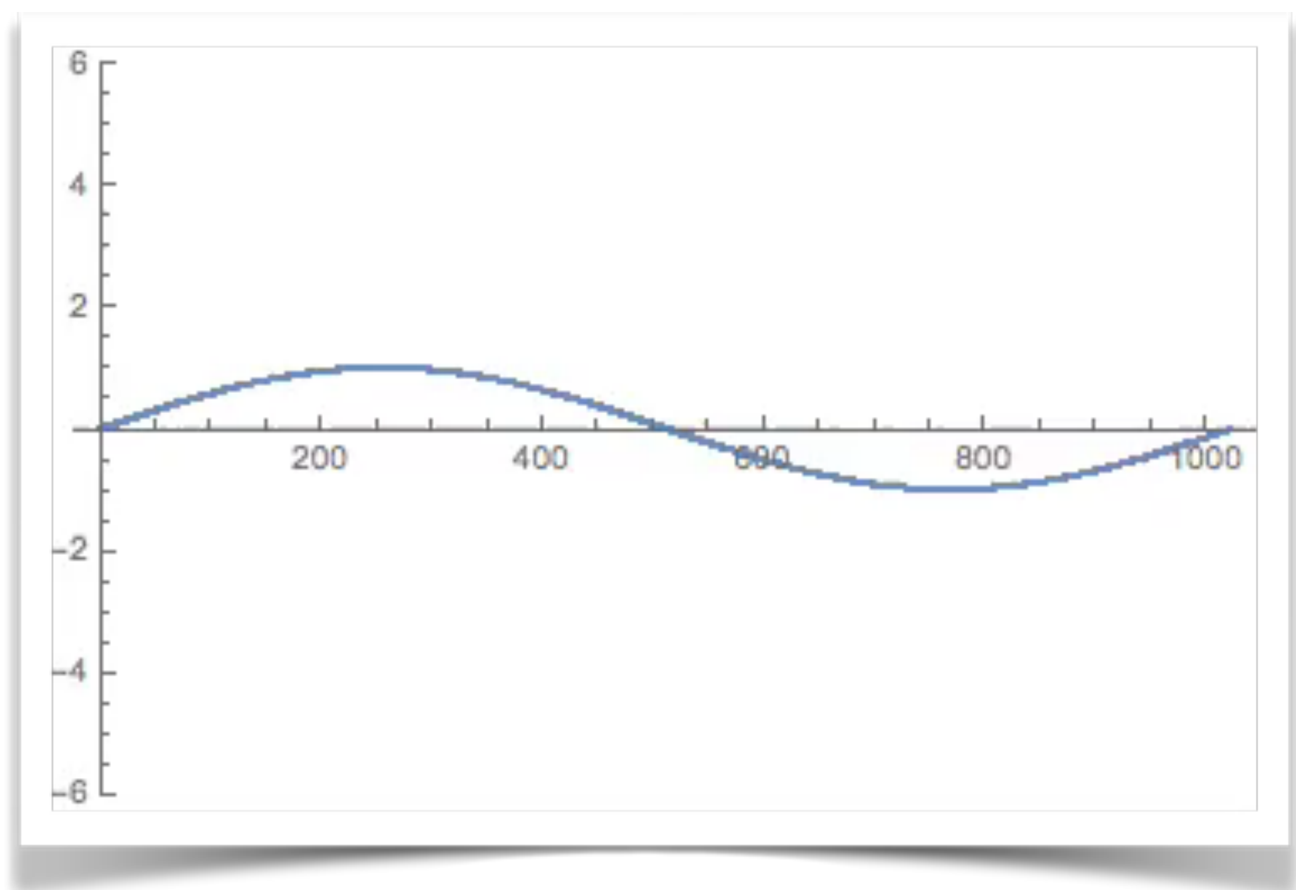

Single QFD shock

The Green function for Schrödinger's equation $i\partial_t\psi = -\frac{\epsilon}{2}\partial_{xx}\psi$ reads

$$G_0(x,t|x_0,t_0) = \sqrt{\frac{1}{2i\pi m(t-t_0)}}\, e^{\frac{i(x-x_0)^2}{2\epsilon(t-t_0)}}$$

The shock solution thus reads

$$\psi(\mathbf{x},t) = \int_{-\infty}^{\infty} dy\, \sqrt{\frac{1}{2i\pi\epsilon t}}\, e^{\frac{i}{\epsilon}\left(\frac{(y-x)^2}{2t}+\cos(y)\right)} \tag{1}$$

In the $\epsilon \to 0$ limit, this integral can be computed by using Pearcey's integral defined by

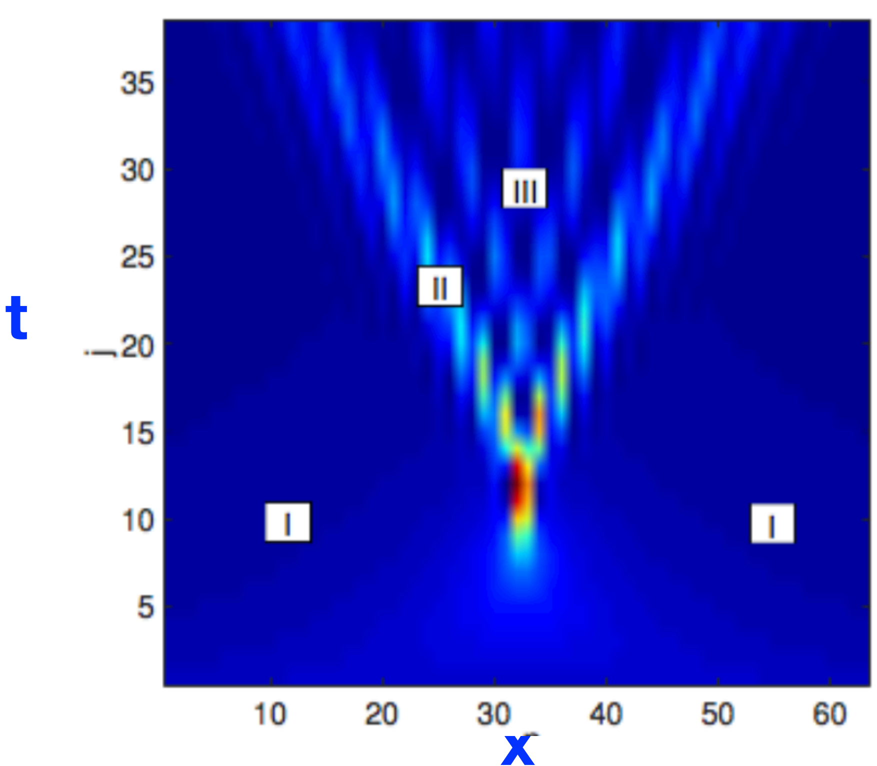

$$I_{\mathcal{P}}(T,X) = \int_{-\infty}^{\infty} dy\, e^{i\left(Xy+Ty^2+y^4\right)}$$

Asymptotic expressions can be readily obtained

see refs. in https://arxiv.org/abs/1709.10417

Some orders of magnitude

See e.g. Galantucci, Baggaley, Barenghi, Krstulovic, Eur. Phys. J. Plus (2020) 135:547
for a detailed discussion of the orders of magnitude

Here I only want to mention:

- Helium phase diagram
- Landau's 2-fluid model
- Characteristic length: system size, inter vortex distance, coherence length, excitations mean free path
- characteristic speeds: first and second sound speed
- viscosity

Existing models

- HBVK
- 3D Vortex Line/Navier-Stokes coupled simulations

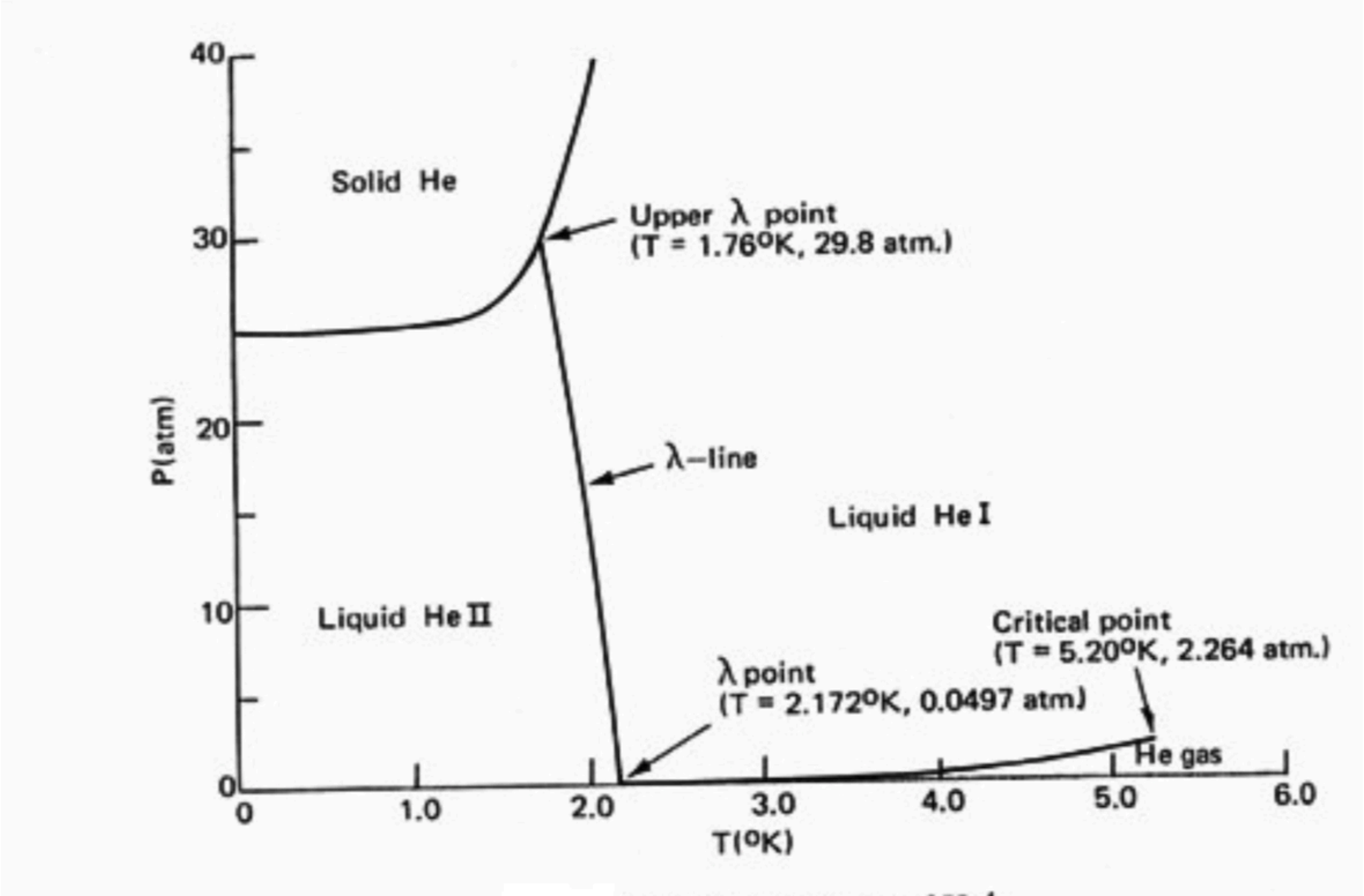

Models?

Can a GP-NS model be quantitatively applied to describe two-fluid helium quantum flows?

First, in order to correctly describe superfluid liquid helium, we need a correct equation of state and a dispersion relation also involving rotons excitations. This implies that the GP equation needs to be extended by including non-local and higher order nonlinear terms.

Second, the NS description itself for the normal fluid will be valid only for scales of the order, or smaller than the thermal excitation mean free path.

A quantitative self-consistent description of the two-fluid helium flow for all range of temperatures is still an open problem.

Physical motivations

- Recent experimental results have produced visualizations of the motion of the normal fluid in systems where it is coupled to the superfluid vortices by mutual friction
- Producing and imaging a thin line of He2∗ molecular tracers in helium-4, J. Gao, A. Marakov, W. Guo, B. T. Pawlowski, S. W. Van Sciver, G. G. Ihas, D. N. McKinsey, and W. F. Vinen, Review of Scientific Instruments 86, 093904 (2015)

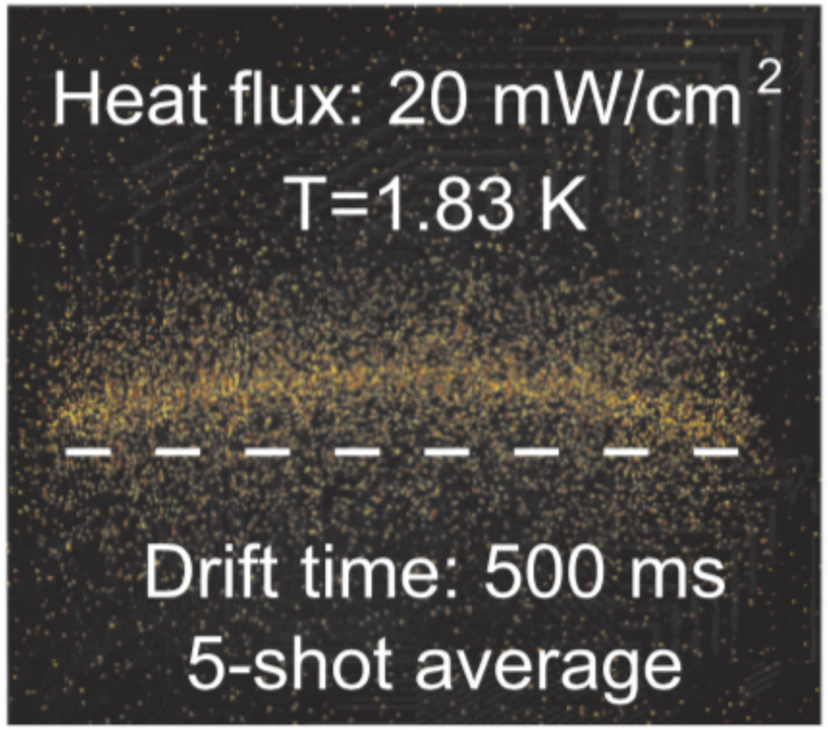

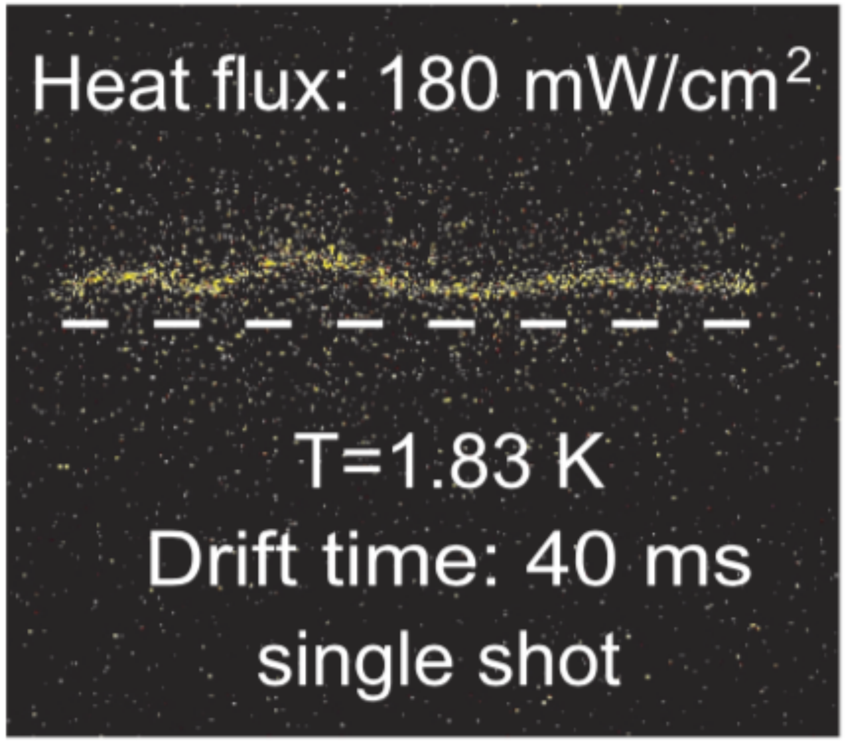

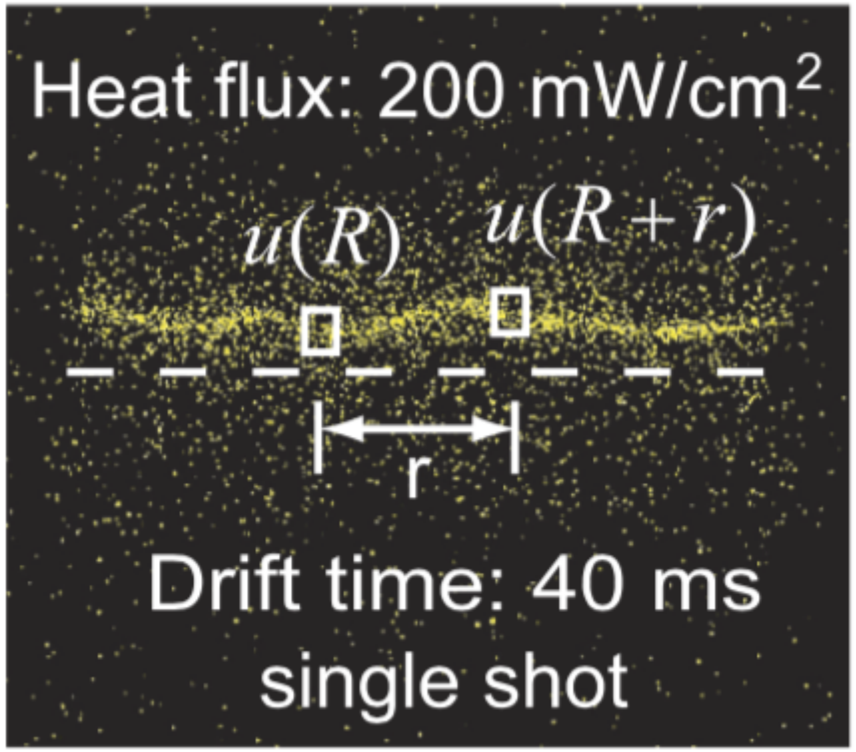

Physical motivations

- Motivated by the experimental results of J. Gao people are now doing 3D Vortex Line/Navier-Stokes coupled simulations: Galantucci, A. W. Baggaley, C. F. Barenghi, G. Krstulovic, Eur. Phys. J. Plus, 135:547 (2020)
- Vortex Line/Lattice Boltzmann coupled simulations have also been recently performed: Sosuke Inui and Makoto Tsubota Phys. Rev. B 104, 214503 (2021)
- Next 3 slides: method and some typical results obtained with these VL/NSE and VL/LBE models

LV/NSE method: PRF 8, 014702 (2023)

II. MODEL AND NUMERICAL EXPERIMENT

Our model builds on the vortex filament (VF) theory of Schwarz [18], a widely used approach [19,20] which describes vortex lines as space curves $\mathbf{s}(\xi, t)$ of infinitesimal thickness moving according to

$$\boxed{\dot{\mathbf{s}}(\xi, t) = \frac{\partial \mathbf{s}}{\partial t} = \mathbf{v}_s + \alpha \mathbf{s}' \times \mathbf{v}_{ns} - \alpha' \mathbf{s}' \times (\mathbf{s}' \times \mathbf{v}_{ns}),} \tag{1}$$

where $\mathbf{s}' = \partial \mathbf{s}/\partial \xi$, $\mathbf{v}_{ns} = \mathbf{v}_n - \mathbf{v}_s$ at $\mathbf{s}$, α and α' are temperature-dependent friction coefficients [21], $\mathbf{v}_n$ is the normal fluid velocity at $\mathbf{s}$, and $\mathbf{v}_s$ is the superfluid velocity induced at $\mathbf{s}$ by the entire vortex configuration $\mathcal{L}$ via

$$\boxed{\mathbf{v}_s(\mathbf{s}, t) = \frac{\kappa}{4\pi} \oint_{\mathcal{L}} \frac{\mathbf{s}_1'(\xi_1, t) \times [\mathbf{s} - \mathbf{s}_1(\xi_1, t)]}{|\mathbf{s} - \mathbf{s}_1(\xi_1, t)|^3} d\xi_1 .} \tag{2}$$

The original VF model consists of Eqs. (1) and (2) and an algorithm to perform vortex reconnections. Its limitation is that the normal fluid velocity $\mathbf{v}_n$ is imposed *a priori*, neglecting the backreaction of the superfluid vortex lines on $\mathbf{v}_n$. Recent experiments [22,23] suggest that normal fluid wakes may form behind each individual vortex line. To account for this effect, which is crucial to understand quantized vortex bundles, we couple Eqs. (1) and (2) self-consistently with the Navier-Stokes equations for $\mathbf{v}_n$ supplemented with a mutual friction force $\mathbf{F}_{ns}$:

$$\frac{\partial \mathbf{v}_n}{\partial t} + (\mathbf{v}_n \cdot \nabla)\mathbf{v}_n = -\frac{1}{\rho}\nabla p_n + \nu_n \nabla^2 \mathbf{v}_n + \frac{\mathbf{F}_{ns}}{\rho_n}, \tag{3}$$

$$\mathbf{F}_{ns} = \oint_{\mathcal{L}} \mathbf{f}_{ns}(\mathbf{s})\delta(\mathbf{x} - \mathbf{s}) d\xi, \quad \nabla \cdot \mathbf{v}_n = 0. \tag{4}$$

VL/NSE result

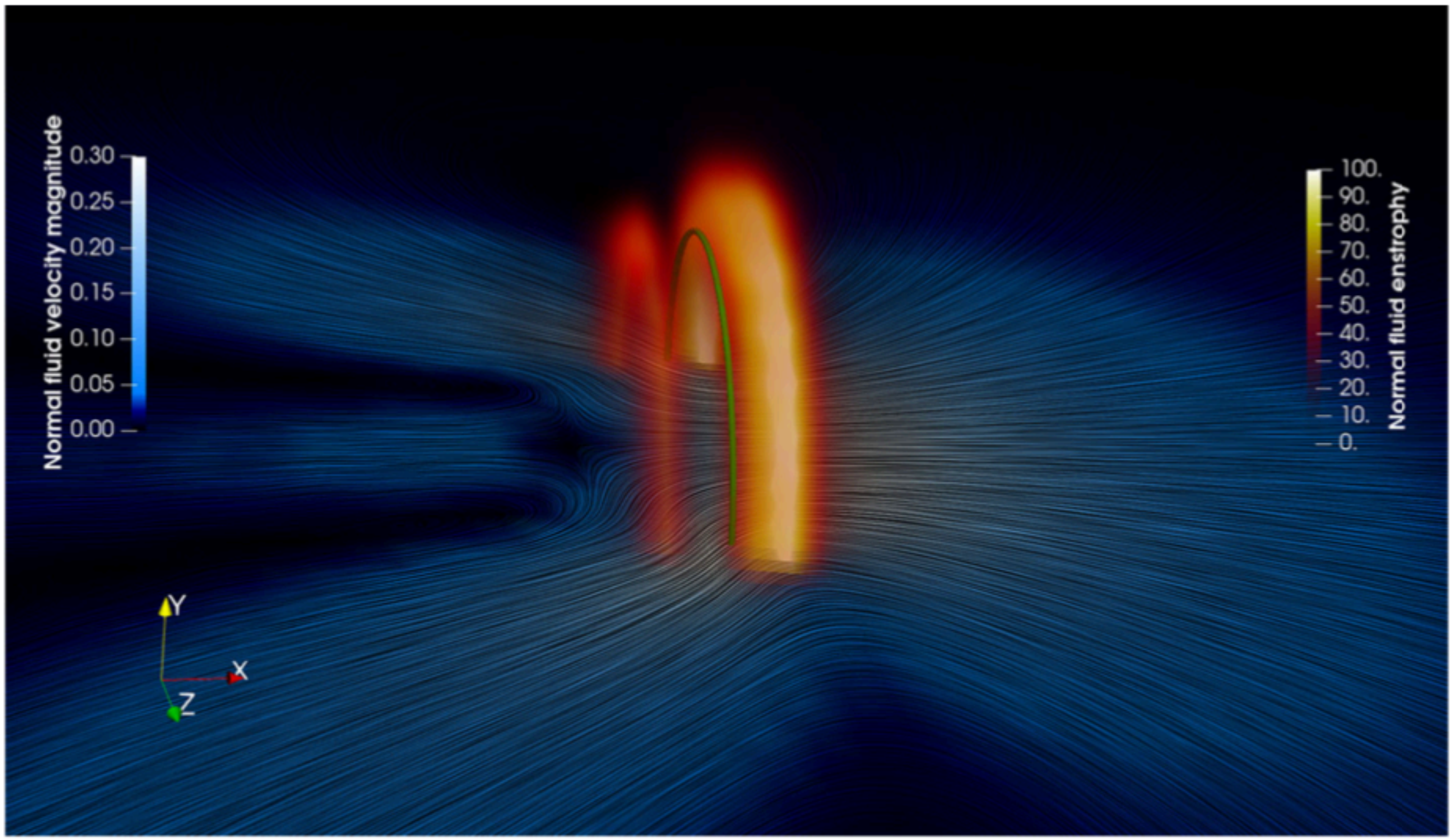

Fig. 7 A superfluid vortex ring moving in the normal fluid initially at rest. Half of the superfluid vortex ring is visible as a green line intersecting the xy plane; the superfluid vortex ring moves to the right along the x direction. The normal fluid enstrophy is displayed by the orange–reddish–black rendering: two concentric normal fluid vortex rings are visible, slightly ahead and slightly behind the superfluid vortex ring, travelling in the same direction. The normal fluid velocity magnitude is also displayed using a black-blue-white rendering on the xy plane

VL/LBE result

COUPLED DYNAMICS OF QUANTIZED VORTICES AND ... PHYSICAL REVIEW B **104**, 214503 (2021)

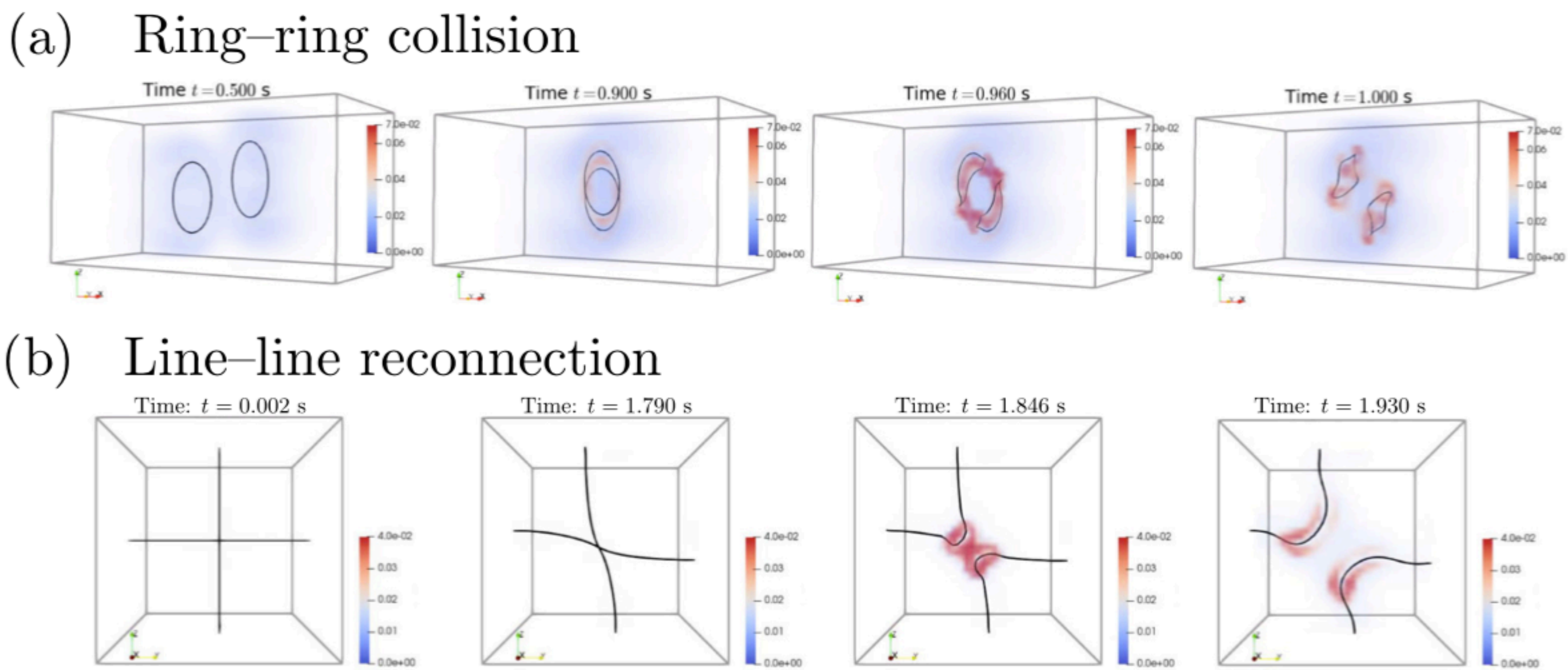

FIG. 3. (a), (b) Snapshots of vortex reconnection events and normal-fluid vorticity distribution: (a) Collision of two vortex rings and (b) vortex reconnection between two linear vortices. In each panel, the regions with low vorticity are set to be transparent such that the high-vorticity region (in red) can be easily observed.

GPE for the superfluid?

- Idea: replace the Line vortex model by a Gross-Pitaevskii model
- Interest: quantized vortex reconnection is described without any phenomenological approximation
- Drawback: GPE needs to resolve the coherent length (that is taken to be 0 in line vortex) so we'll have much less scale-separation than in a VLM

Standard (uncoupled) GPE and NSE

GPE

$$\boxed{i\hbar\frac{\partial\psi}{\partial t} = -\frac{\hbar^2}{2m}\nabla^2\psi + g|\psi|^2\psi,}$$

Madelung $\psi(\mathbf{x},t) = \sqrt{\frac{\rho(\mathbf{x},t)}{m}}\exp\left(i\frac{m}{\hbar}\phi(\mathbf{x},t)\right)$, $\rho(\mathbf{x},t)$ is the mass density

fluid velocity $\mathbf{v} = \frac{\hbar}{m}\nabla\phi$.

the vorticity $\omega = \nabla\times\mathbf{v}$ is given by $\omega(\mathbf{r}) = \frac{h}{m}\int ds\frac{d\mathbf{r}_0}{ds}\delta(\mathbf{r}-\mathbf{r}_0(s)),$

Bogoliubov $\omega_B(k) = \sqrt{\frac{g\mathbf{k}^2|\Psi_0|^2}{m} + \frac{\hbar^2\mathbf{k}^4}{4m^2}}$. $c = \sqrt{g|\Psi_0|^2/m}$. $\xi = \frac{\hbar}{\sqrt{2gm|\Psi_0|^2}}$.

Incompressible NSE

$$\boxed{\begin{aligned}\partial_t\mathbf{v} + (\mathbf{v}\cdot\nabla)\mathbf{v} &= -\frac{1}{\rho}\nabla p + \nu\nabla^2\mathbf{v},\\ \nabla\cdot\mathbf{v} &= 0,\end{aligned}}$$

Previous attempts to couple NES and GPE

- There was a single attempt (to the best of our knowledge): C. Coste,The European Physical Journal B - Condensed Matter and Complex Systems, 1, pp 245–253 (1998)

- The context is the Landau compressible 2 fluid model without vortices (First and Second sound, Fountain Effect, etc.)

- Our context is different: mutual friction on GPE vortices and incompressible NSE

Building up the model

We need:

- 1) An expression for the vortex line velocity induced by the GPE dynamics that is regular on the lines
- 2) Expressions for (a) the GPE lines slip velocity and (b) the volume force on the normal fluid
- 3) Implement the line slip velocity in the GPE

Regularized superfluid velocity

$$\mathbf{v}_s^\epsilon(\mathbf{r}) = \frac{i\hbar}{2m}\frac{\psi\nabla\overline{\psi} - \overline{\psi}\nabla\psi}{\overline{\psi}\psi + \epsilon^2\overline{\rho}_s},$$

$$\mathbf{v}_s^{reg} = (1+\epsilon^2)\,\mathcal{F}^{-1}\left(e^{-\frac{k^2}{k_{\rm reg}^2}}\mathcal{F}(\mathbf{v}_s^\epsilon)\right),$$

$$\mathbf{\Omega} = \nabla\times\mathbf{v}_s^{reg}$$

$$F^{-1} = \frac{\hbar}{2m}\frac{1}{\pi}\left[\int_{-\infty}^{\infty} e^{-\frac{k^2}{k_{\rm reg}^2}}\,dk\right]^2 = \frac{\hbar}{2m}\,k_{\rm reg}^2.$$

We finally define the 'normalized' vorticity field

$$\hat{\mathbf{\Omega}} = F\mathbf{\Omega} = F\nabla\times\mathbf{v}_s^{reg},$$

which has a norm that is maximum and close to 1 on the vortex line and much smaller than 1 away from the vortex line.

Slip velocity and friction force

The Magnus force density caused by $\mathbf{v}_{\text{slip}}$ can be estimated starting from the momentum conservation equation (Sonin, 1997):

$$\boxed{\mathbf{F}_{MD} = \rho_s \, \mathbf{v}_{\text{slip}} \times (\nabla \times \mathbf{v}_s^{reg}).} \tag{19}$$

This force density must be opposite to the force density acting on the NS fluid, thus

$$\boxed{\mathbf{F}_{MD} = -\mathbf{F}_{SN}.} \tag{20}$$

For $\mathbf{F}_{SN}$ we start from the simple phenomenological expression considering a force with longitudinal and transversal components

$$\boxed{\mathbf{F}_{SN} \sim \rho_n \left[\beta s' \times (s' \times (\mathbf{v}_n - \mathbf{v}_L)) + \beta' s' \times (\mathbf{v}_n - \mathbf{v}_L) \right],} \tag{21}$$

Slip velocity and friction force

where ρ_n and $\mathbf{v}_n$ are the density and velocity of the normal fluid, $\mathbf{v}_L$ the velocity of the vortex line, s' the unit tangent to the line (see Fig. 1), and β, β' two phenomenological coefficients.

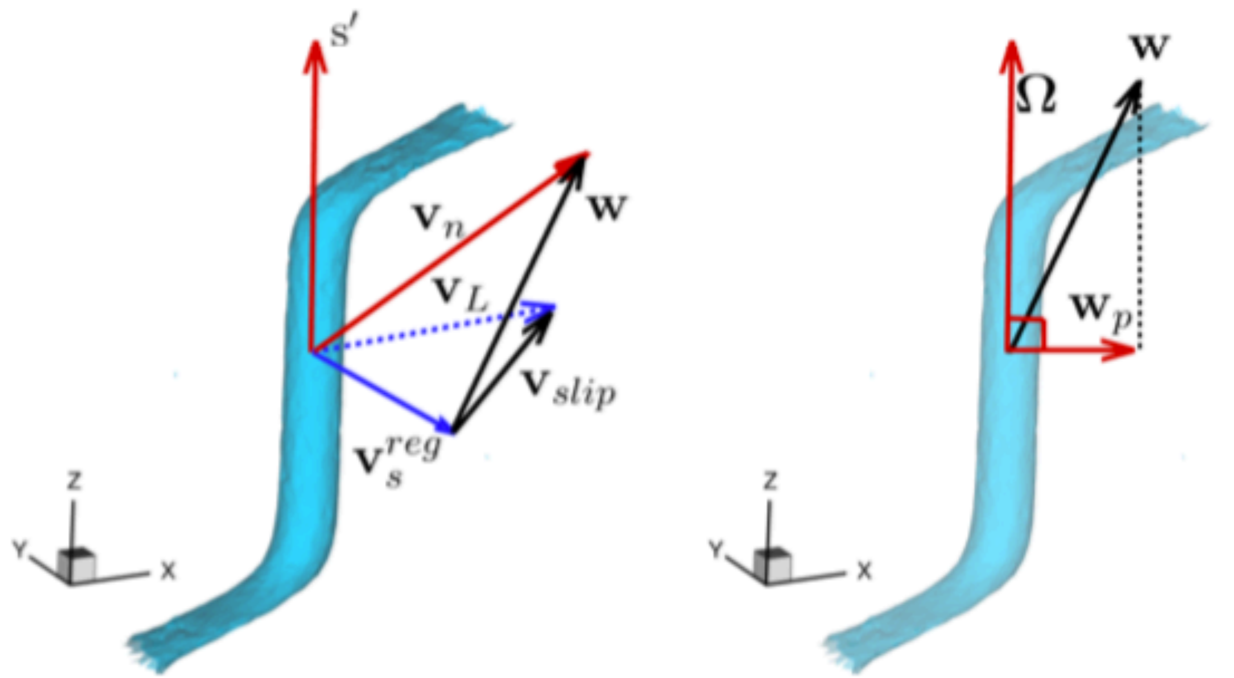

Figure 1: Sketch of velocities acting on a vortex line.

- $\boldsymbol{v}_s^{reg}$ the regularized superfluid velocity,
- $\boldsymbol{v}_L$ the vortex velocity,
- $\boldsymbol{v}_{\text{slip}} = \boldsymbol{v}_L - \boldsymbol{v}_s$ the slip velocity,
- $\mathbf{w} = \boldsymbol{v}_n - \boldsymbol{v}_s^{reg}$ the counterflow,
- $\mathbf{w}_p = \mathbf{w} - \frac{\mathbf{w}\cdot\boldsymbol{\omega}_s}{\boldsymbol{\omega}_s\cdot\boldsymbol{\omega}_s}\boldsymbol{\omega}_s$ the counterflow perpendicular to the vortex line.

Using the fact that **on vortex lines** the vector $\hat{\boldsymbol{\Omega}} = F\boldsymbol{\Omega}$ is of norm 1 and directed along the line, we postulate the following formula for the volume force, equivalent to Eq. (21):

$$\mathbf{F}_{SN} = \rho_n \left[B_\star (\nabla \times \mathbf{v}_s^{reg}) \times (F(\nabla \times \mathbf{v}_s^{reg}) \times (\mathbf{v}_n - \mathbf{v}_L)) + B'_\star (\nabla \times \mathbf{v}_s^{reg}) \times (\mathbf{v}_n - \mathbf{v}_L) \right], \tag{22}$$

Slip velocity and friction force

then the equation $\mathbf{F}_{MD} = -\mathbf{F}_{SN}.$ **yields:**

$$\boxed{\mathbf{v}_{\text{slip}} = U_\star \mathbf{w}_p + V_\star \hat{\mathbf{\Omega}} \times \mathbf{w},}$$

$$\boxed{\mathbf{F}_{SN} = \rho_s\, \mathbf{\Omega} \times (U_\star \mathbf{w}_p + V_\star \hat{\mathbf{\Omega}} \times \mathbf{w}).}$$

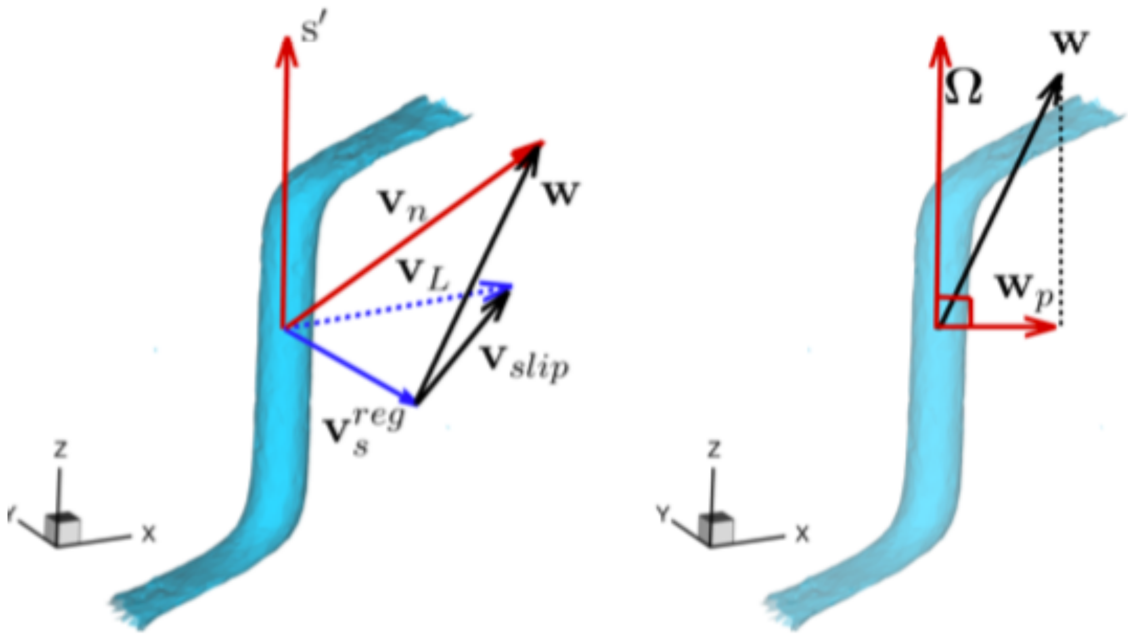

with:

$$\boxed{\begin{aligned} U_\star &= \frac{\rho_n \left(B_\star^2 |\hat{\mathbf{\Omega}}|^2 \rho_n + B_\star' \left(\rho_s + \rho_n B_\star'\right)\right)}{B_\star^2 |\hat{\mathbf{\Omega}}|^2 \rho_n^2 + \left(\rho_s + \rho_n B_\star'\right)^2}, \\ V_\star &= \frac{B_\star \rho_n \rho_s}{B_\star^2 |\hat{\mathbf{\Omega}}|^2 \rho_n^2 + \left(\rho_s + \rho_n B_\star'\right)^2}. \end{aligned}}$$

Implementing the slip velocity in GPE

$$\boxed{\mathbf{v}_{\text{slip}} = U_\star \mathbf{w}_p + V_\star \hat{\boldsymbol{\Omega}} \times \mathbf{w},}$$

the first term is parallel to w and the second is perpendicular

$$\boxed{\mathbf{F}_{SN} = \rho_s\, \boldsymbol{\Omega} \times (U_\star \mathbf{w}_p + V_\star \hat{\boldsymbol{\Omega}} \times \mathbf{w}).}$$

the first term corresponds to a NSE force perpendicular to w and the second to an NSE force parallel to w

So, in the case of a vortex ring moving in a zero-velocity normal fluid the first term that changes the speed of the ring should not transfer energy from GPE to NSE but the second that shrinks the ring and produces a NSE force in the direction of the motion should transfer energy.

Conserving way to implement slip

- Consider a vortex set at the origin: $\psi_v = R(r)e^{\pm i\theta}$, solution of $-\frac{\hbar^2}{2m}\nabla^2\psi_v + g|\psi_v|^2\psi_v = 0$.
- A vortex moving at speed $\boldsymbol{U}^{\mathrm{adv}}$ is obtained through the transformation $\psi(\boldsymbol{x}, t) = \psi_v(\boldsymbol{x} - t\boldsymbol{U}^{\mathrm{adv}})$ and is solution of:

$$\frac{\partial\psi}{\partial t} + \boldsymbol{U}^{\mathrm{adv}} \cdot \nabla\psi = i\left(\frac{\hbar}{2m}\nabla^2\psi - \frac{g}{\hbar}|\psi|^2\psi\right).$$

- This term is obtained through the substitution $\nabla \to \nabla + \frac{i}{2\alpha}\boldsymbol{v}$ that was proposed by Coste, *Nonlinear Schrödinger equation and superfluid hydrodynamics*, Eur. Phys. J. B, 1998.
- The energy is conserved.

Non-conserving way to implement slip

- Consider the velocity $\boldsymbol{U}_{\perp}^{\mathrm{adv}} = \hat{\boldsymbol{\omega}}_s \times \boldsymbol{U}^{\mathrm{adv}}$.
- And the dynamics:

$$\frac{\partial\psi}{\partial t} - i\boldsymbol{U}_{\perp}^{\mathrm{adv}} \cdot \nabla\psi = i\left(\frac{\hbar}{2m}\nabla^2\psi - \frac{g}{\hbar}|\psi|^2\psi\right).$$

- For short times the vortex is moving with speed $\boldsymbol{U}^{\mathrm{adv}}$.
- the Energy is dissipated.

Using both conserving and non-conserving ways

$$\boxed{\mathbf{v}_{\text{slip}} = U_\star \mathbf{w}_p + V_\star \hat{\boldsymbol{\Omega}} \times \mathbf{w},}$$

- Idea: let's use both approaches with the following advection velocities:

$$\begin{cases} \boldsymbol{U}^{\text{adv}} & = U_\star \mathbf{w}_p \quad \text{conservative}, \\ \boldsymbol{U}_\perp^{\text{adv}} & = \dfrac{\hat{\boldsymbol{\omega}}_s}{|\hat{\boldsymbol{\omega}}_s|} \times V_\star \hat{\boldsymbol{\omega}}_s \times \mathbf{w} = -V_\star |\hat{\boldsymbol{\omega}}_s| \mathbf{w}_p \quad \text{non-conservative}. \end{cases}$$

complex-valued $\boldsymbol{v}_{\text{slip}}$ in the substitution $\nabla \to \nabla + \frac{i}{2\alpha} \boldsymbol{v}$

$$\boxed{\mathbf{v}_{\text{slip}}^{cpl} = (U_\star + iV_\star |\hat{\boldsymbol{\Omega}}|) \mathbf{w}_p.}$$

Numerical form of the model

$$\begin{aligned}\partial_t \mathbf{v}_n + (\mathbf{v}_n \cdot \nabla)\mathbf{v}_n &= -\frac{1}{\rho_n}\nabla p + \nu_n \nabla^2 \mathbf{v}_n + \frac{1}{\rho_n}\mathbf{F}_{SN},\\ \nabla \cdot \mathbf{v}_n &= 0,\end{aligned}$$

$$\mathbf{F}_{SN} = \rho_s \left(\nabla \times \mathbf{v}_s^{reg}\right) \times \left(U_\star \mathbf{w}_p + V_\star \hat{\boldsymbol{\Omega}} \times \mathbf{w}\right),$$

with $\mathbf{w} = \mathbf{v}_n - \mathbf{v}_s^{reg}$, $\mathbf{w}_p = \mathbf{w} - \frac{\mathbf{w}\cdot\hat{\boldsymbol{\Omega}}}{|\hat{\boldsymbol{\Omega}}|^2}\hat{\boldsymbol{\Omega}}$ and $U_\star$ and $V_\star$ given by

$$\mathbf{v}_s^{\epsilon}(\mathbf{r}) = \frac{i\hbar}{2m}\frac{\psi\nabla\overline{\psi} - \overline{\psi}\nabla\psi}{\overline{\psi}\psi + \epsilon^2\overline{\rho}_s},$$

$$\mathbf{v}_s^{reg} = (1+\epsilon^2)\,\mathcal{F}^{-1}\left(e^{-\frac{k^2}{k_{\rm reg}^2}}\mathcal{F}(\mathbf{v}_s^{\epsilon})\right),$$

$$\begin{aligned}U_\star &= \frac{\rho_n\left(B_\star^2|\hat{\boldsymbol{\Omega}}|^2\rho_n + B'_\star\left(\rho_s + \rho_n B'_\star\right)\right)}{B_\star^2|\hat{\boldsymbol{\Omega}}|^2\rho_n^2 + \left(\rho_s + \rho_n B'_\star\right)^2},\\ V_\star &= \frac{B_\star\rho_n\rho_s}{B_\star^2|\hat{\boldsymbol{\Omega}}|^2\rho_n^2 + \left(\rho_s + \rho_n B'_\star\right)^2}.\end{aligned}$$

$$\begin{aligned}\partial_t\psi &= i\left(\alpha\nabla^2\psi - \gamma(|\psi|^2 - \overline{\rho}_s)\psi - \frac{1}{\alpha}\frac{(\mathbf{v}_{\rm slip}^{cpl})^2}{4}\psi\right)\\ &- (\mathbf{v}_{\rm slip}^{cpl}\cdot\nabla)\psi - \frac{1}{2}(\nabla\cdot\mathbf{v}_{\rm slip}^{cpl})\psi\\ &+ \eta_D(\alpha\nabla^2\psi - \gamma(|\psi|^2 - \overline{\rho}_s)\psi + \mu\psi).\end{aligned}$$

$$\mathbf{v}_{\rm slip}^{cpl} = (U_\star + iV_\star|\hat{\boldsymbol{\Omega}}|)\mathbf{w}_p.$$

Numerical form of the model

The final system of coupled equations (48) and (50) is advanced in time using a fourth-order Runge-Kutta method (with implicit discretization of Laplacian operators). Fourier-spectral space discretization is used for both equations. The coupling algorithm was implemented in the framework of the modern parallel (MPI-OpenMP) numerical code called GPS (Gross-Pitaevskii Simulator) (Parnaudeau et al., 2015). The GPS code was initially designed as a spectral parallel solver for the GP equation using various time-integration methods (Strang splitting, relaxation, Crank-Nicolson). It was recently used to simulate quantum turbulent flows (Kobayashi et al., 2021). The Navier-Stokes solver was added to the GPS code using standard Fourier pseudo-spectral method (Gottlieb and Orszag, 1977). Only one external library, FFTW (Frigo and Johnson, 2005), was required for the computation.

Model coefficient

The coupling model has several coefficients that have to be fixed accordingly to the physics or be adjusted numerically.

To give the model a physical background, the friction coefficients $U_\star$ and $V_\star$ can be linked to tabulated experimental friction coefficients used in the physical literature for helium II

The model also includes a few numerical coefficients that have to be prescribed: the two smoothing parameters ε^2 and k_{reg} used in the definition of v^{reg} , and the dissipation coefficient η.

On dimensional grounds, ε^2 has to be proportional to ϱ_s,

k_{reg} to ξ^{-1} (the inverse of the healing length) and

η_D to the physical friction coefficient B_{tab}.

They will be adjusted by numerical tests reproducing the evolution of quantized vortices in a normal fluid.

Fixing the parameters on 2D vortex pairs

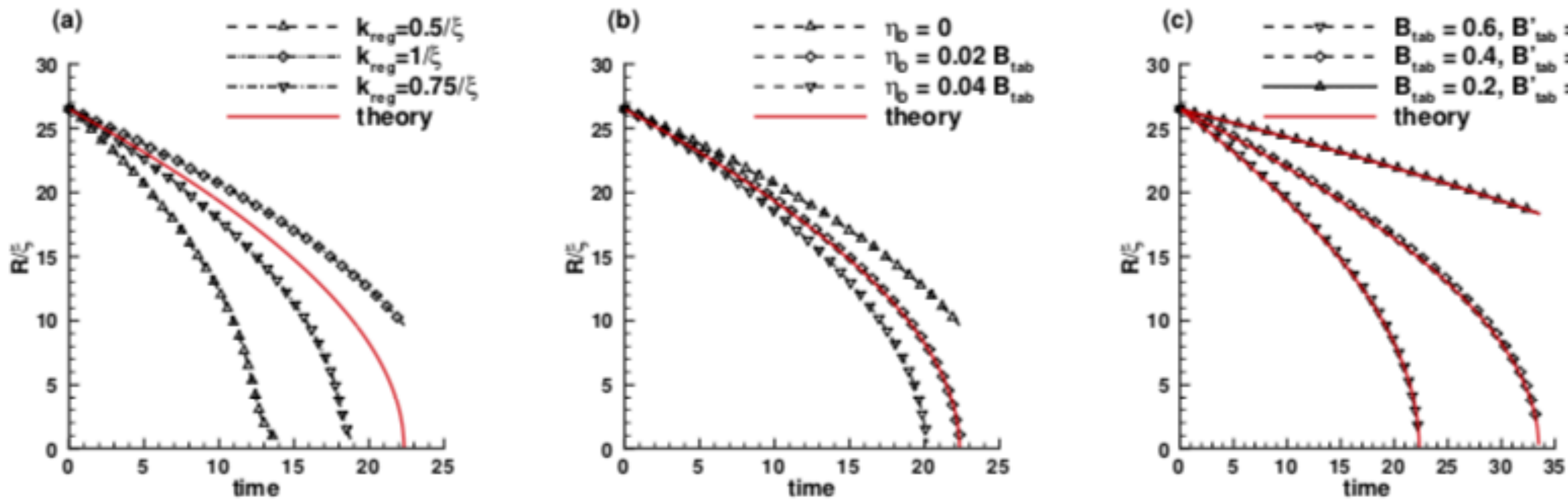

Figure 2: 2D evolution of a superfluid vortex dipole. One-way GP-NS coupling, with $\mathbf{u}_n = 0$. Time evolution of the half distance between the two vortices normalized by the size of the vortex core ξ. Solid lines represent the analytical solution. (a) Results for three values of of the smoothing wave number $k_{\rm reg}$ and common values $B_{tab} = 0.6$ and $B'_{tab} = 0.1$. (b) Results for three values of the dissipation parameter η_D and common values $B_{tab} = 0.6$ and $B_{tab} = 0.1$. (c) Results for $k_{\rm reg} = 1/\xi$, $\eta_D = 0.02 B_{tab}$, and three different choices for the coupling force parameters B_{tab} and B'_{tab}.

Fixing the parameters on 2D vortex pairs

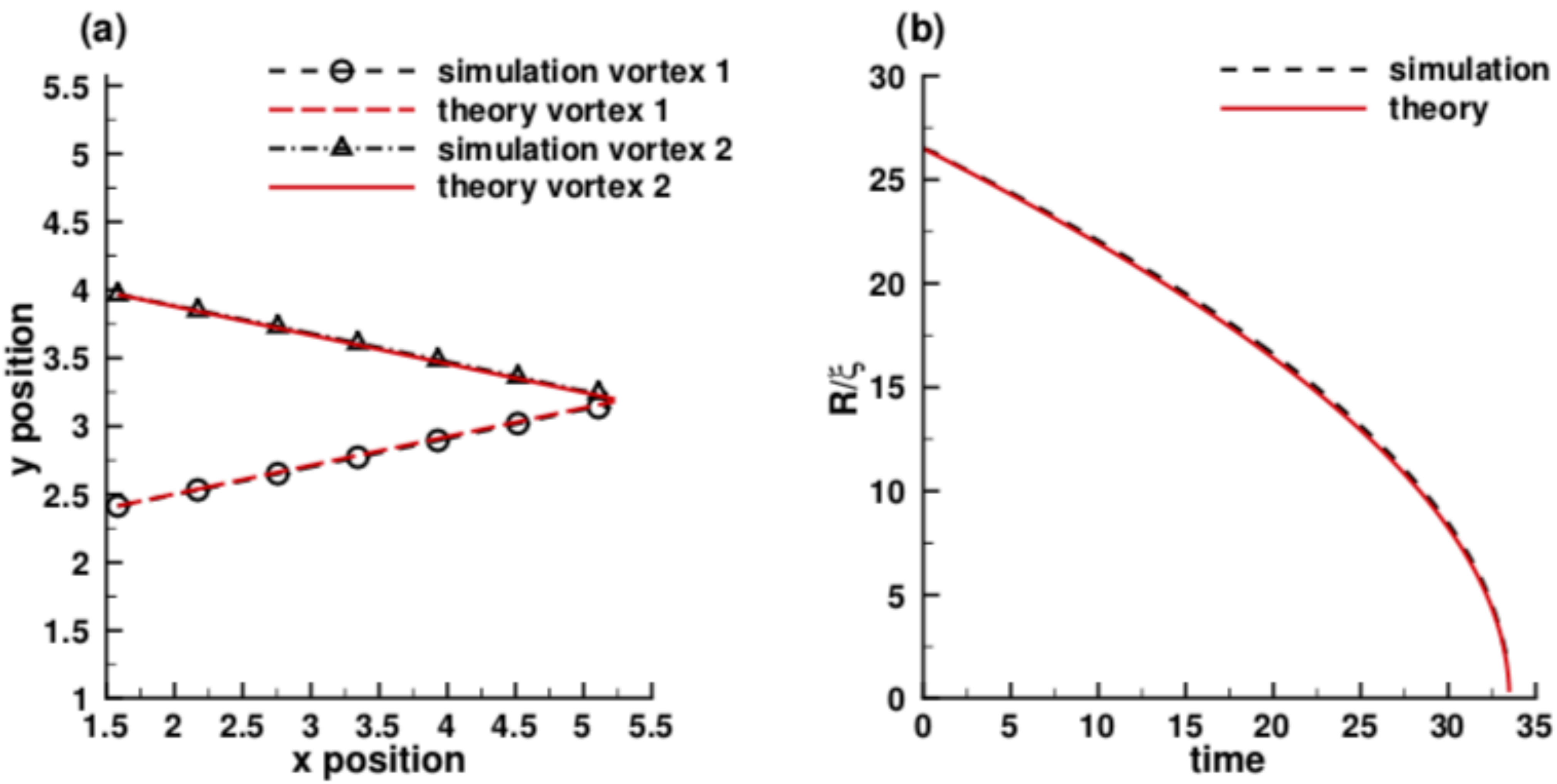

Figure 3: 2D evolution of a superfluid vortex dipole. One-way GP-NS coupling, with $\mathbf{u}_n = 0$. Simulation with fixed parameters: $B_{tab} = 0.4$, $B'_{tab} = 0.1$, $d/\xi = 53$, $N = 256$, $k_{\text{reg}}^{-1} = \xi$, $\eta_D = 0.02B_{tab}$. (a) Trajectories of the two vortices. (b) Time evolution of the the half distance between the two vortices normalized by the size of the vortex core.

Effect of one-way two-way coupling

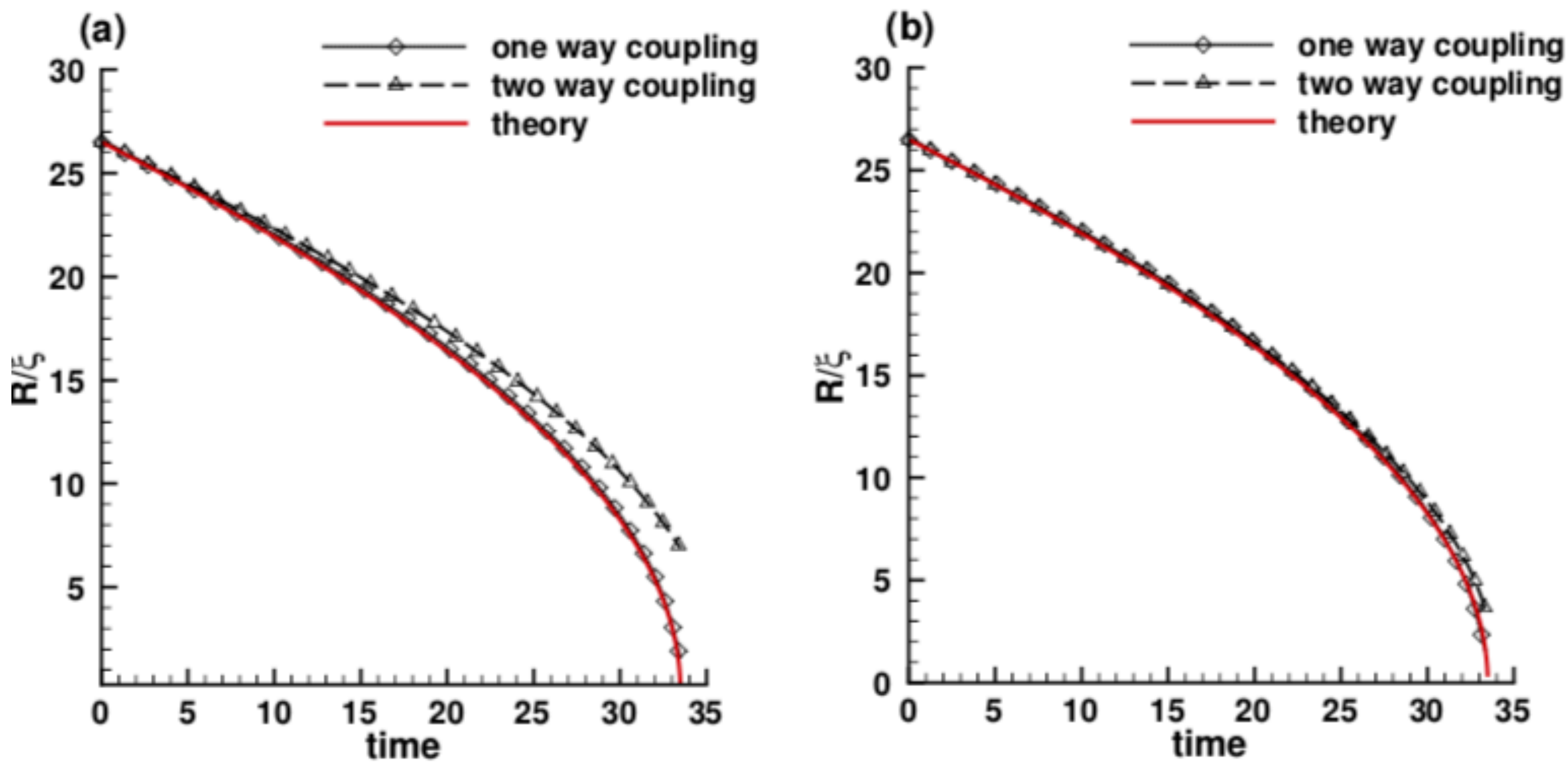

igure 4: 2D evolution of a superfluid vortex dipole. Time evolution of the alf distance between the two vortices normalized by the size of the vortex ore ξ. Comparison between $(-\diamond-)$ one-way coupling $(\mathbf{u}_n = 0)$ and $(-\triangle-)$ wo-way coupling $(\mathbf{u}_n \neq 0)$ for different physical parameters (a) : $B_{tab} =$ .4, $B'_{tab} = 0.1$, $\eta_D = 0.02 B_{tab}$, (b) : $B_{tab} = 0.4$, $B'_{tab} = 0.4$, $\eta_D = 0.01 B_{tab}$. ommon parameters of the model: $d/\xi = 53$, $N = 256$, $k_{\text{reg}}^{-1} = \xi$.

Two way coupling

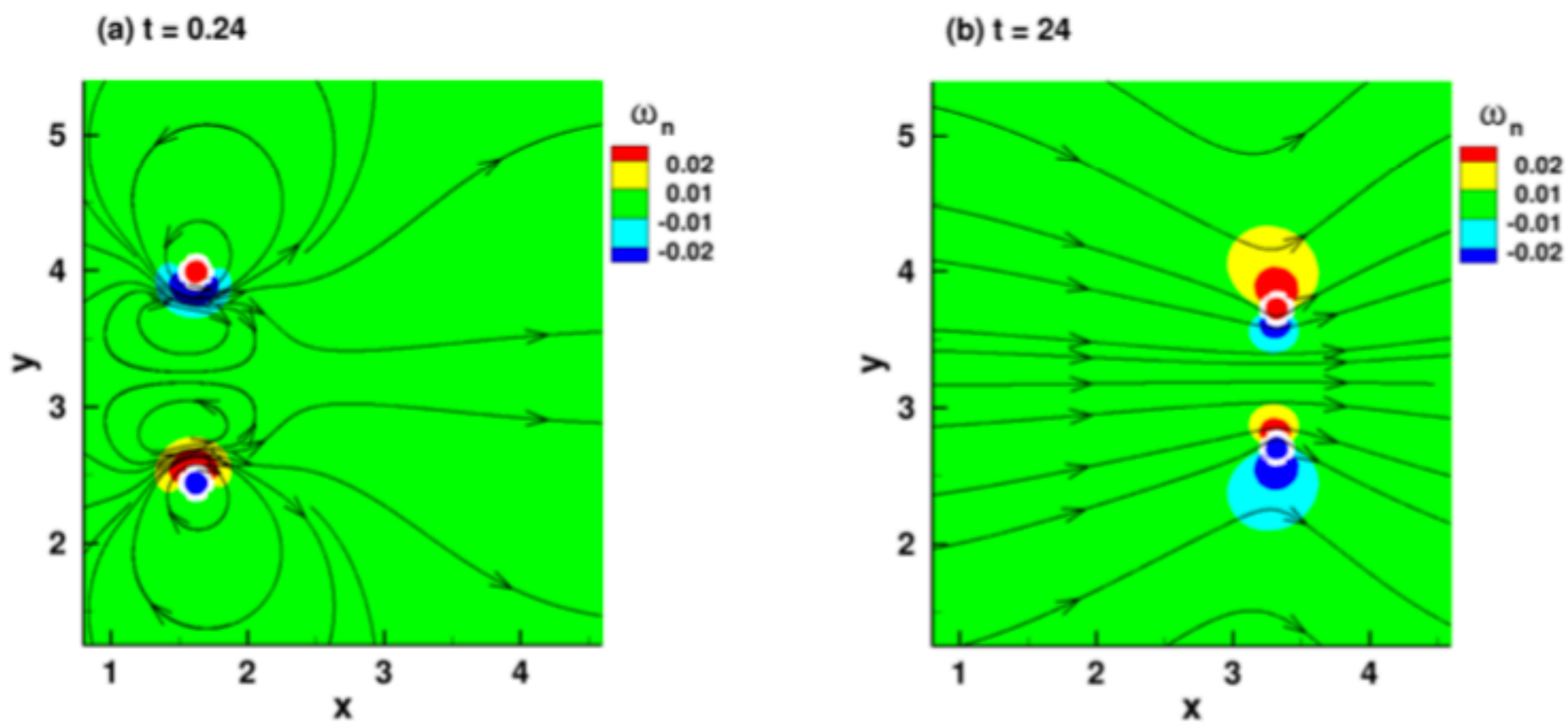

Figure 5: 2D evolution of a superfluid vortex dipole. Two-way GP-NS coupling. Illustration of the triple-vortex structure of the flow. The entrained normal fluid is represented by its vorticity contours (colors) and streamlines (arrow black lines). Superfluid vortices (white circles) are identified by an iso-contour of low atomic density ($0.5\ |\psi|^2_{max}$). Snapshots of the flow for time instants: (a) t=0.24, (b) t=24. Parameters of the simulation: $B_{tab} = 0.4$, $B'_{tab} = 0.1$, $\eta_D = 0$, $d/\xi = 53$, $N = 256$, $k_{\rm reg}^{-1} = \xi$.

2D superfluid vortex pair

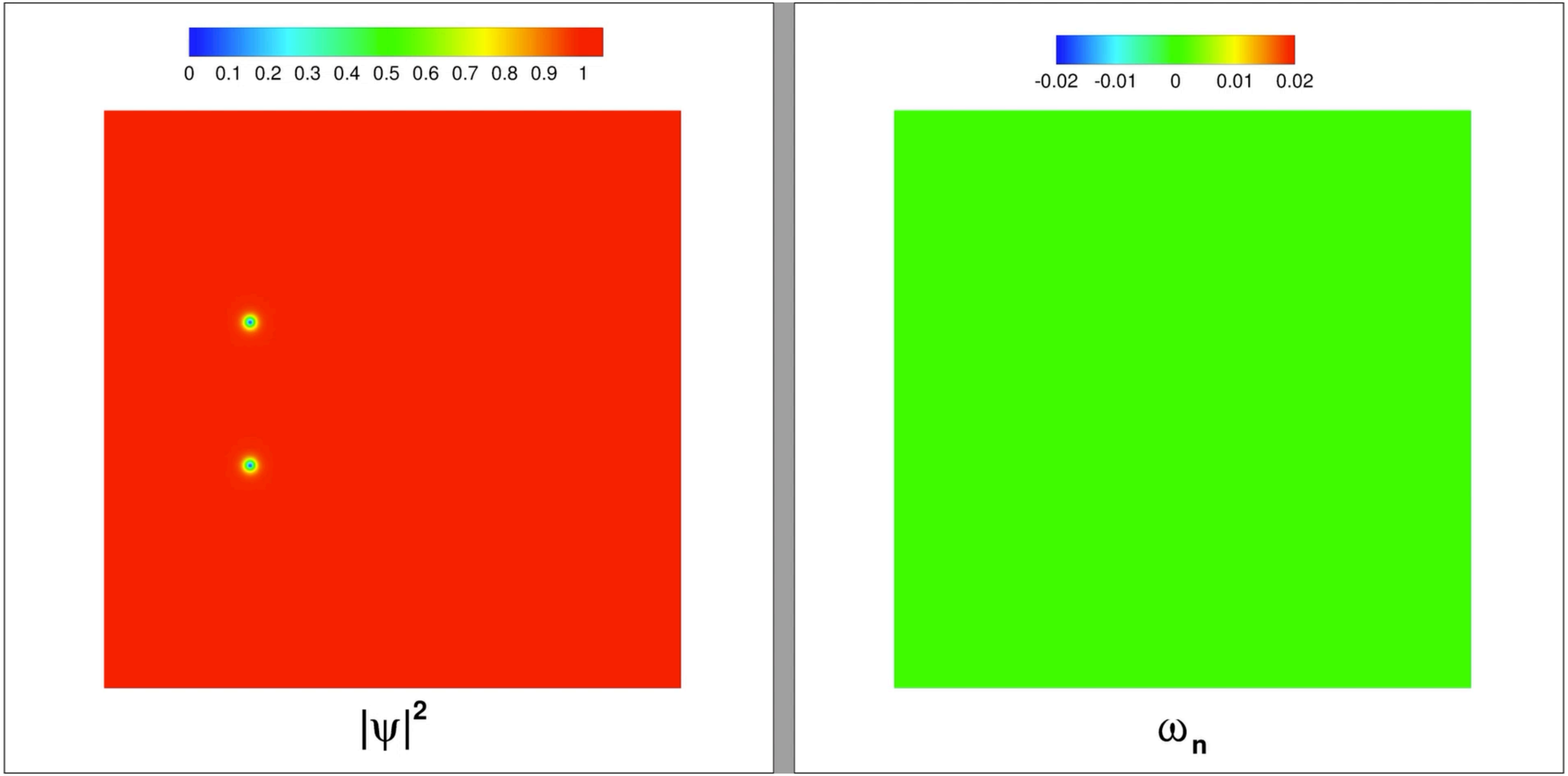

3D vortex rings

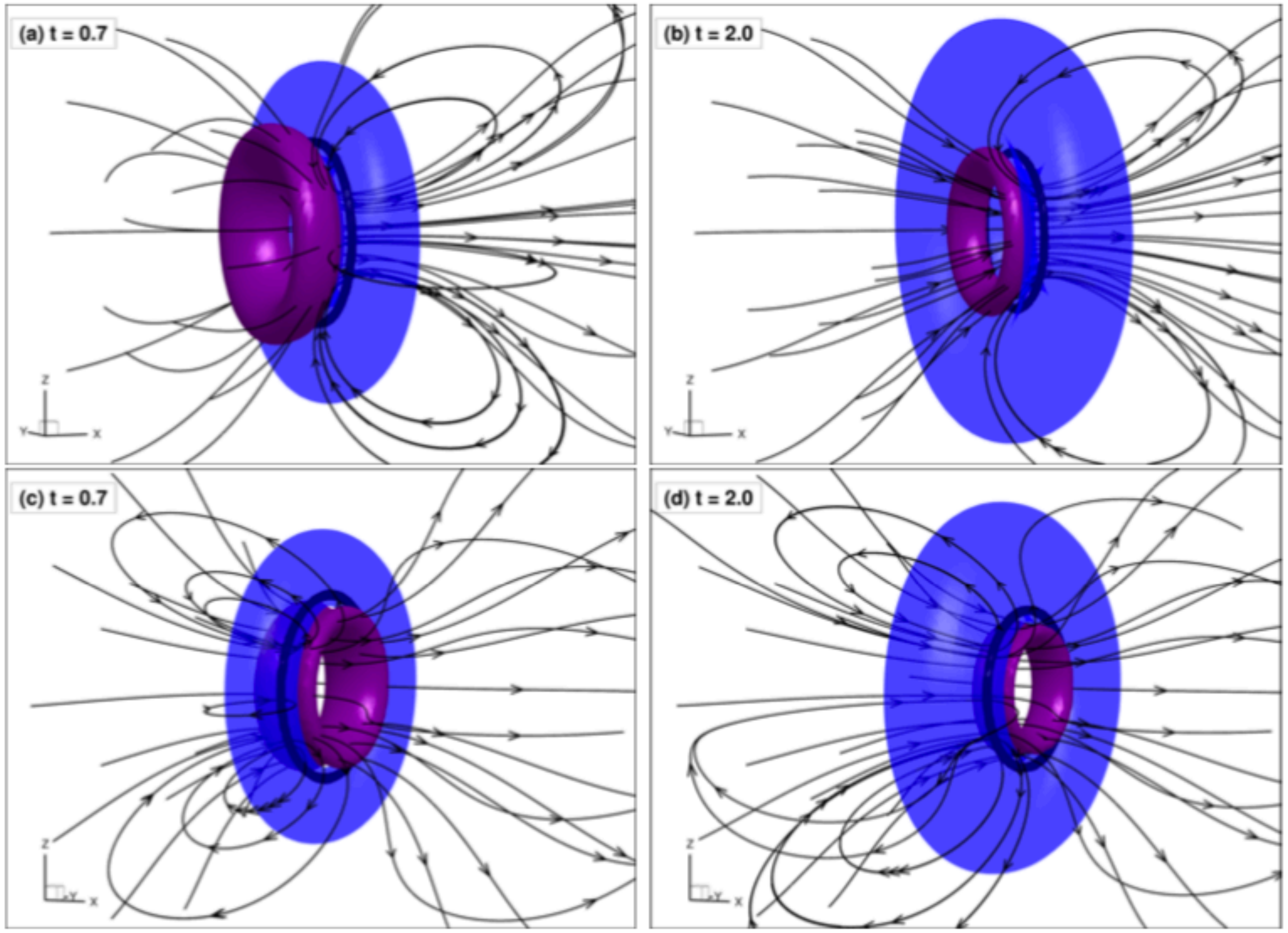

Figure 6: 3D evolution of a superfluid vortex ring in a normal fluid initially at rest. Snapshots for two time instants. Physical parameters $\rho_n/\rho_s = 1$, $B_{tab} = B'_{tab} = 0.4$, $\eta_D = 0.035 B_{tab}$ (panels a, b), $B_{tab} = 0.4 > B'_{tab} = 0.1$, $\eta_D = 0.05 B_{tab}$ (panels c, d). Illustration of the triple-vortex structure. The superfluid vortex ring (in black) is identified by an iso-surface of low atomic density ($0.5\ |\psi|^2_{max}$). The two counter-rotating normal vortex rings are identified by iso-surfaces of normal fluid azimuthal vorticity: 0.03 for the blue outer ring and (-0.03) for the red inner ring. The streamlines in the normal fluid are also drawn. Mesh resolution 128^3.

3D superfluid vortex ring

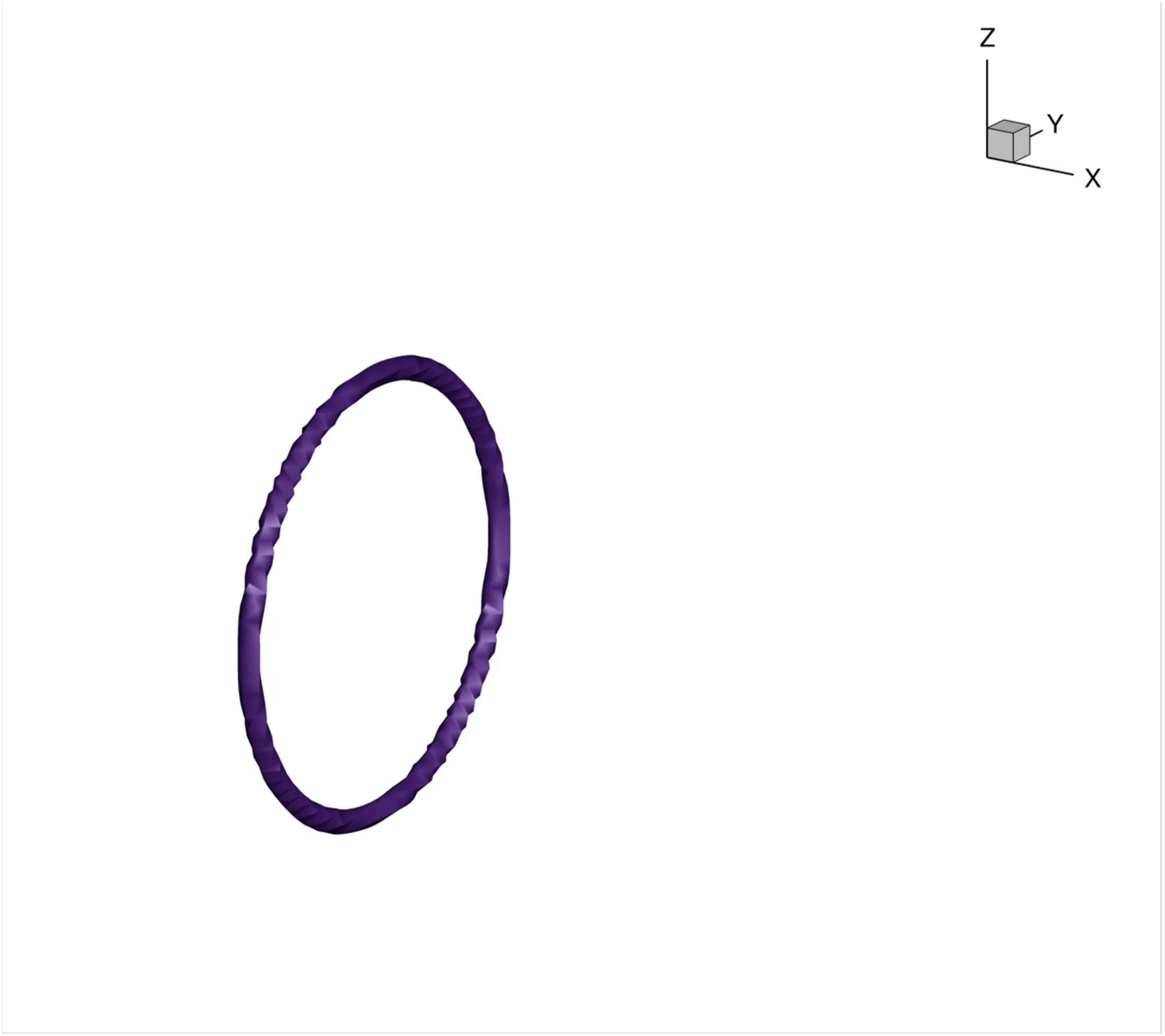

Reconnection

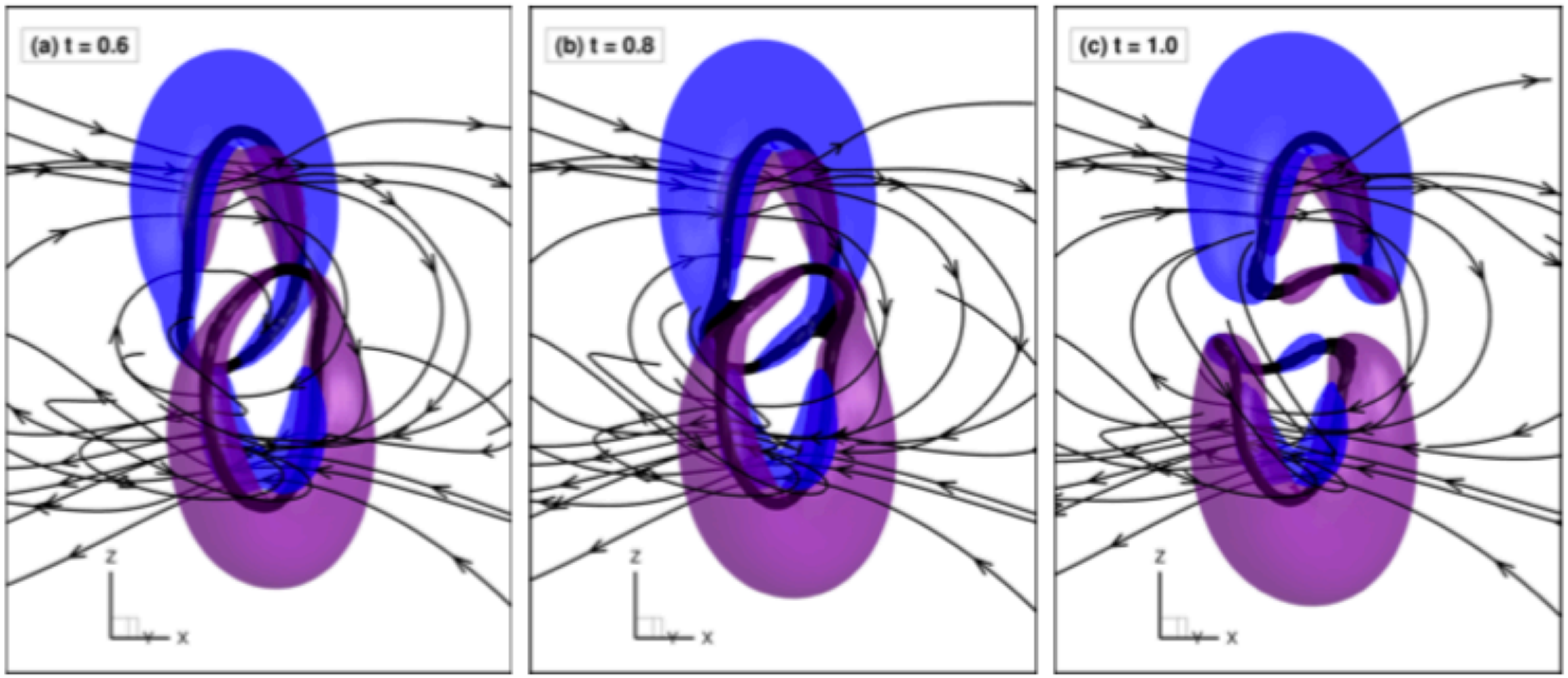

Figure 7: 3D head-on collision of two superfluid vortex ring in a normal fluid initially at rest. Snapshots for three time instants. Physical parameters $\rho_n/\rho_s = 1$, $B_{tab} = 0.4$, $B'_{tab} = 0.1$, $\eta_D = 0.05B_{tab}$. Illustration of the structure of vortex reconnection. The superfluid vortex ring (in black) is identified by an iso-surface of low atomic density $(0.2\ |\psi|^2_{max})$. The two counter-rotating normal vortex rings are identified by iso-surfaces of normal fluid azimuthal vorticity: 0.05 for the blue outer ring and (-0.05) for the red inner ring. The streamlines in the normal fluid are also drawn. Mesh resolution 128^3.

Reconnection

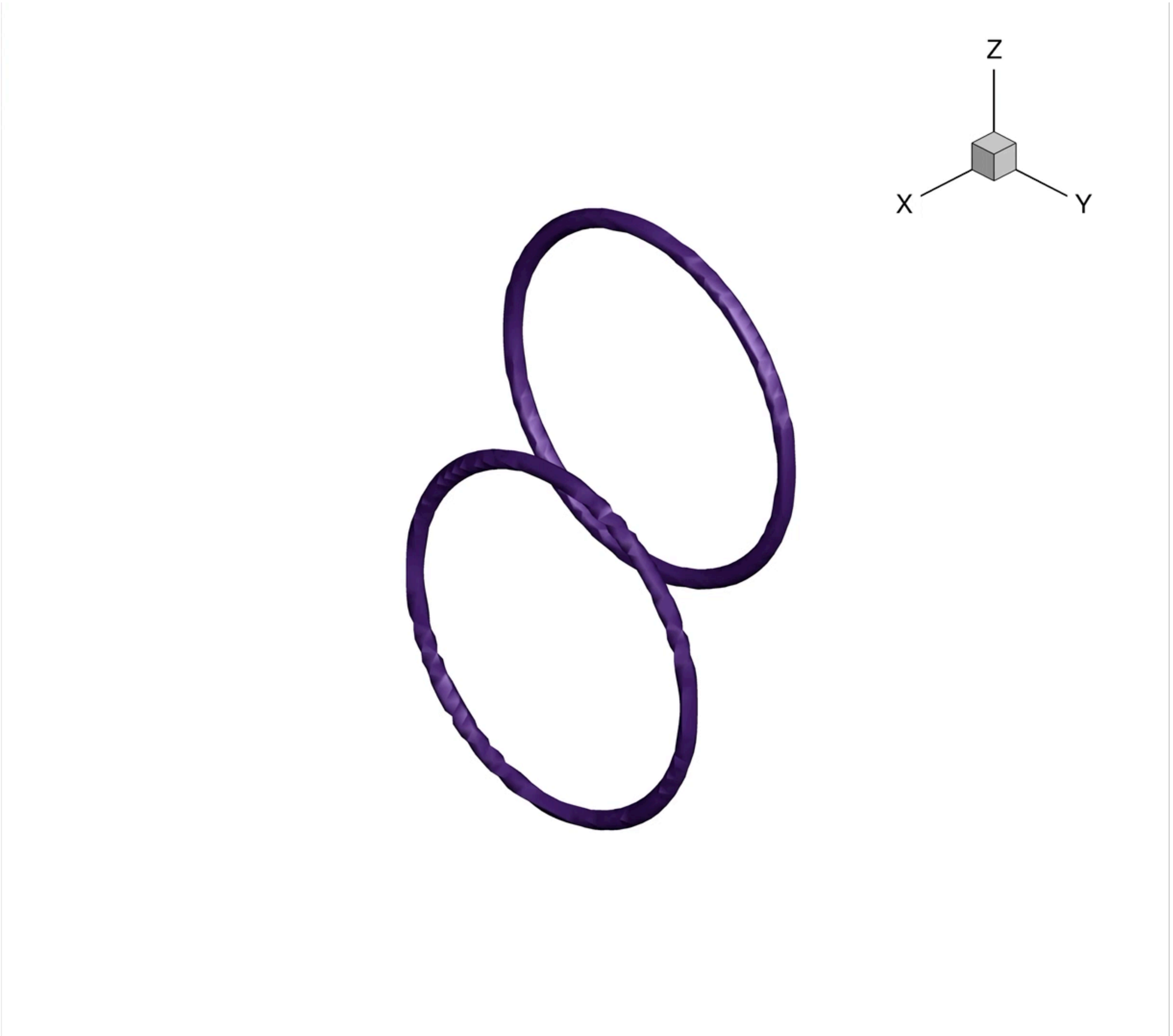

Conclusion

- The simulation of superfluid vortex rings head-on collision proved the ability of the method to account, without any phenomenological assumption, on the complex vortex interaction and reconnection.

- This new numerical model offers the possibility to revisit many fundamental phenomena established using the vortex filament method for superfluids (see Tsubota et al. (2017)): reconnections of superfluid vortex lines in a NS fluid, movement of superfluid vortex bundles in a normal fluid, counter-flow quantum turbulence and, finally, two-fluid quantum turbulence.

Thank you!